Supplemental material for

"*Inter-regional dependence of J-REIT stock prices: A heteroscedasticity-robust time series approach*"

Kaiji Motegi* – Kobe University

Yoshitaka Iitsuka† – Kobe University

This draft: September 12, 2022

1 Details on the J-REIT selection process

As of February 5, 2021, there are 62 Japanese real estate investment trusts (J-REITs) listed on the Tokyo Stock Exchange (TSE) Real Estate Investment Trust Securities Market. In the main paper, we selected central and local J-REITs for each of the office, residential, and hotel sectors. In this supplemental material, we provide complete details on the selection process of these companies. On Japan REIT DB maintained by Prop Tech plus Inc., there are 6 property types: office, residential, hotel, commercial, logistics, and others. Table 1 indicates which J-REIT specializes in which property type, where "specialization" is defined as individual properties of a single sector accounting for 80% or more of the total appraisal value of a portfolio. The number of sector-specific J-REITs is 12 for office, 6 for residential, 6 for hotel, 3 for commercial, 9 for logistics, and 1 for others (i.e., #44 HCM specializing in healthcare properties). These 37 J-REITs account for 59.7% of the total appraisal value of the market, indicating that the majority of J-REITs specialize in a single property type. A practical advantage of the property-type specialization is that the maintenance and operation cost can be reduced (Capozza and Seguin, 1999).

* *Corresponding author*. Graduate School of Economics, Kobe University. Address: 2-1 Rokkodai-cho, Nada, Kobe, Hyogo 657-8501 Japan. E-mail: motegi@econ.kobe-u.ac.jp

† Graduate School of Economics, Kobe University. E-mail: 200e501e@stu.kobe-u.ac.jp

The regional decompositions of the office, residential, and hotel J-REITs are listed in Table 1 of the main paper. For these sectors, the selection process of the central and local J-REITs are fully explained in Section 3.1 of the main paper. In Table 2 of this supplemental material, regional decompositions of the 3 commercial and 9 logistics J-REITs are shown. Below we explain why a suitable pair of central and local J-REITs cannot be found for these sectors.

Recall that Japan REIT DB has 6 regional classifications: (1) Tokyo5: Central five wards of Tokyo (i.e., Chiyoda, Chuo, Minato, Shinjuku, and Shibuya). (2) Tokyo23: The twenty-three wards of Tokyo excluding Tokyo5. (3) TokyoP: Tokyo Prefecture excluding Tokyo23. (4) Kanto: Kanto Area excluding TokyoP (i.e., Chiba, Gumma, Ibaraki, Kanagawa, Saitama, and Tochigi Prefectures). (5) Chubu & Kinki: Chubu Area (i.e., Aichi, Fukui, Gifu, Ishikawa, Nagano, Niigata, Shizuoka, Toyama, and Yamanashi Prefectures) and Kinki Area (i.e., Hyogo, Kyoto, Mie, Nara, Osaka, Shiga, and Wakayama Prefectures). (6) Others: Others not classified above.

All 3 commercial J-REITs heavily invest in Kanto, Chubu & Kinki, or Others: 65.3% for #03 JMF, 68.7% for #11 FRI, and most notably 100% for #37 ARI (Table 2). Hence, it is impossible to select from them central and local J-REITs which have non-overlapping regional allocations. The same problem arises in the logistics sector, where the total share of Kanto, Chubu & Kinki, and Others is at least 76.0% recorded by #13 JLF. An extreme example is #59 IAL, whose individual properties are all located in Kanto. There is a strong tendency that the commercial and logistics J-REITs own individual properties outside Tokyo, which makes it hard to find a pair of central and local companies. Thus, the commercial and logistics sectors are excluded from the main analysis.

2 Details on the preliminary data analysis

As explained in Section 3.1 of the main paper and Section 1 of this supplemental material, we decided to analyze the six J-REIT securities:

Central office J-REIT: #26 Mori Hills REIT Investment Corporation (MHR).

Local office J-REIT: #36 One REIT, Inc. (ORI).

Central residential J-REIT: #33 Comforia Residential REIT, Inc (CRR).

Local residential J-REIT: #45 Samty Residential Investment Corporation (SRIC).

Central hotel J-REIT: #54 MORI TRUST Hotel Reit, Inc. (MTH).

Local hotel J-REIT: #52 Ooedo Onsen Reit Investment Corporation (OOR).

Due to the data availability, the whole sample period was chosen to be February 7, 2017 – March 11, 2022 (1244 business days); see Section 3.2 of the main paper for detailed explanations. In Figures 1-3 of the main paper, time series plots of the log-price and log-return series are drawn for the six selected shares. We found through these figures that February 27 – May 1, 2020 is a period of extreme turbulence due to the COVID-19 pandemic. Hence, we decided to split the whole sample period into three sub-periods:

Pre-crisis period: February 7, 2017 – February 26, 2020 (745 days).

Crisis period: February 27 – May 1, 2020 (45 days).

Post-crisis period: May 7, 2020 – March 11, 2022 (454 days).

In Figure 1 of this supplemental material, we draw time series plots for all 62 J-REIT securities as well as the TSE REIT Index for completeness. We observe from Figure 1 that the COVID-19 crisis hit all securities simultaneously, which supports our choice of the crisis period (February 27 – May 1, 2020). All shares experienced extreme turbulence during the crisis period, confirming that the COVID-19 pandemic affected the entire J-REIT market.

To further inspect the impacts of the pandemic on each share, we report sample statistics of the daily log-return of each share during the crisis period in Table 3. Not surprisingly, the mean and median of the log-return are negative for most shares. The minimum value ranges from -0.323 of #46 NMF to -0.078 of #29 SPI. This implies that all shares experienced at least a 7.8% price drop on some day during the crisis period, highlighting the wide-spreading impact of the pandemic. The maximum value ranges from 0.093 of #29 SPI to 0.240 of #26 MHR, the central office J-REIT. The standard deviation ranges from 0.036 of #29 SPI to 0.082 of #22 JEI, indicating that volatility surged for all shares during the crisis. The kurtosis ranges from 3.208 of #35 HRR to 10.81 of #34 NPR. Overall, Table 3 suggests that the six shares we selected are nothing exceptional; the impacts of the pandemic on them are not particularly large or small compared with other shares.

3 Heteroscedasticity-robust methods

In this section, we describe the procedures of the heteroscedasticity-robust methods adopted in our main analysis. To make this section self-contained, we briefly review the notation and model in the main paper. Let (P_{1t}, P_{2t}) be the stock prices of central and local J-REITs on day $t \in \{1, \dots, T\}$, respectively. Let P_t^m be the level of the TSE REIT Index on day t. The log-price series are defined as $\boldsymbol{Y}_t = (Y_{1t}, Y_{2t}, Z_t)^\top = (\ln P_{1t}, \ln P_{2t}, \ln P_t^m)^\top$. Similarly, the log-return series are defined as follows:

$$\boldsymbol{y}_t = \begin{bmatrix} y_{1t} \\ y_{2t} \\ z_t \end{bmatrix} = \begin{bmatrix} \Delta Y_{1t} \\ \Delta Y_{2t} \\ \Delta Z_t \end{bmatrix} = \begin{bmatrix} \Delta \ln P_{1t} \\ \Delta \ln P_{2t} \\ \Delta \ln P_t^m \end{bmatrix} = \Delta \boldsymbol{Y}_t, \tag{1}$$

where Δ is the first-difference operator (e.g., $\Delta Y_{1t} = Y_{1t} - Y_{1t-1}$).

In Section 2.1 of the main paper, we formulate a vector error correction model (VECM) of dimension $K = 3$, unknown cointegrating rank $r \in \{0, 1, \dots, K\}$, and unknown lag length $p \in \mathbb{N}$ with $\mathbb{N}$ being the set of natural numbers:

$$\Delta \boldsymbol{Y}_t = \boldsymbol{A}_0 + \boldsymbol{\alpha} \left(\boldsymbol{\beta}^\top \boldsymbol{Y}_{t-1} + \boldsymbol{\rho}^\top t \right) + \sum_{k=1}^{p} \boldsymbol{A}_k \Delta \boldsymbol{Y}_{t-k} + \boldsymbol{u}_t, \tag{2}$$

where $\boldsymbol{A}_0$ is $K \times 1$ constant parameters; $\boldsymbol{\alpha}$ is $K \times r$ speed-of-adjustment parameters; $\boldsymbol{\beta}$ is $K \times r$ cointegrating parameters; $\boldsymbol{\rho}$ is $1 \times r$ parameters on the linear time trend inside the cointegrating equation; $\boldsymbol{A}_k$ is $K \times K$ vector autoregressive (VAR) parameters; $\boldsymbol{u}_t$ is $K \times 1$ errors which are allowed to have conditional heteroscedasticity of unknown form.

Given (2), we jointly determine the cointegrating rank r and the lag length p by the heteroscedasticity-robust selection algorithm of Cavaliere, De Angelis, Rahbek, and Taylor (2018). In our data analysis, the resulting optimal values are $(\hat{r}^*, \hat{p}^*) = (0, 1)$, under which (2) reduces to the stationary VAR(1) model for the log-return series:

$$\boldsymbol{y}_t = \boldsymbol{A}_0 + \boldsymbol{A}_1 \boldsymbol{y}_{t-1} + \boldsymbol{u}_t, \qquad t \in \{1, \dots, T\}, \tag{3}$$

where $\boldsymbol{y}_t$ is defined in (1). In Section 3.1 of this supplemental material, the wild-bootstrap Granger causality tests of Hafner and Herwartz (2009, HH2009) are described and applied to our data. In Section 3.2, we describe the residual-based moving-block-bootstrap (MBB) of Brüggemann, Jentsch, and Trenkler (2016, BJT2016), which yields asymptotically valid confidence intervals of impulse response functions (IRFs).

3.1 Wild-bootstrap test for Granger causality

3.1.1 Procedure

Given model (3), consider testing Granger non-causality from the central J-REIT y_1 to the local J-REIT y_2 and vice versa. Let $\boldsymbol{A}_1 = [a_{ij,1}]_{i,j}$, then y_1 does not Granger-cause y_2 at horizon $h = 1$ *if and only if* $a_{21,1} = 0$. Similarly, y_2 does not Granger-cause y_1 at $h = 1$ *if and only if* $a_{12,1} = 0$. Such a single zero restriction can be tested via a Wald test, but a robust p-value is needed when $\boldsymbol{u}_t$ is allowed to be conditionally heteroscedastic. The wild-bootstrap p-value of HH2009 is asymptotically valid under the conditionally heteroscedastic error of unknown form. We focus on model (3) to keep notation simple, although the procedure of HH2009 works for any lag length $p \in \mathbb{N}$.

Model (3) can be rewritten as $\boldsymbol{X} = \boldsymbol{A}\boldsymbol{W} + \boldsymbol{U}$, where $\boldsymbol{X} = (\boldsymbol{y}_1, \dots, \boldsymbol{y}_T)$, $\boldsymbol{A} = (\boldsymbol{A}_0, \boldsymbol{A}_1)$, $\boldsymbol{W} = (\boldsymbol{w}_0, \dots, \boldsymbol{w}_{T-1})$, $\boldsymbol{w}_t = (1, \boldsymbol{y}_t^\top)^\top$, and $\boldsymbol{U} = (\boldsymbol{u}_1, \dots, \boldsymbol{u}_T)$. Let $\widehat{\boldsymbol{A}} = (\hat{\boldsymbol{A}}_0, \hat{\boldsymbol{A}}_1)$ be the least squares estimator for $\boldsymbol{A}$, then $\widehat{\boldsymbol{A}} = \boldsymbol{X}\boldsymbol{W}^\top(\boldsymbol{W}\boldsymbol{W}^\top)^{-1}$. Let $\hat{\boldsymbol{U}} = (\hat{\boldsymbol{u}}_1, \dots, \hat{\boldsymbol{u}}_T)$ be the residual, then $\hat{\boldsymbol{U}} = \boldsymbol{X} - \widehat{\boldsymbol{A}}\boldsymbol{W}$. The estimated error covariance matrix is given by $\hat{\boldsymbol{\Sigma}} = T^{-1}\sum_{t=1}^{T} \hat{\boldsymbol{u}}_t\hat{\boldsymbol{u}}_t^\top$. Define $\hat{\boldsymbol{\Gamma}} = T^{-1}\sum_{t=0}^{T-1} \boldsymbol{w}_t\boldsymbol{w}_t^\top$ and $\hat{\boldsymbol{\Omega}} = \hat{\boldsymbol{\Gamma}}^{-1} \otimes \hat{\boldsymbol{\Sigma}}$, where $\otimes$ is the Kronecker product. These matrices will be key components of a Wald test statistic.

Consider the null hypothesis that y_1 does not Granger-cause y_2 at horizon $h = 1$; the opposite direction can be handled analogously. The parametric representation of this hypothesis is $H_0 : a_{21,1} = 0$. Construct a selection matrix $\boldsymbol{R}$ which picks $a_{21,1}$ from $\boldsymbol{a} = \text{vec}(\boldsymbol{A})$, where $\text{vec}(\cdot)$ is the column-wise vectorization operator. Specifically, $\boldsymbol{R}$ is a $1 \times K(K+1)$ vector whose $(K+2)^{th}$ element is 1 and all others are 0. The Wald test statistic associated with H_0 is given by $\hat{\mathcal{W}} = T\hat{\boldsymbol{a}}^\top\boldsymbol{R}^\top(\boldsymbol{R}\hat{\boldsymbol{\Omega}}\boldsymbol{R}^\top)^{-1}\boldsymbol{R}\hat{\boldsymbol{a}}$, where $\hat{\boldsymbol{a}} = \text{vec}(\widehat{\boldsymbol{A}})$.

If the error term $\boldsymbol{u}_t$ is assumed to be serially independent, it can be shown (up to several regularity conditions) that $\hat{\mathcal{W}} \xrightarrow{d} \chi_1^2$ as $T \to \infty$ under H_0. In this case, the asymptotic p-value based on the chi-squared distribution is readily available. Once we allow for conditional heteroscedasticity in $\boldsymbol{u}_t$, the asymptotic chi-squared convergence no longer holds. In this case, the p-value should be computed via the wild bootstrap of HH2009.

The wild bootstrap of HH2009 proceeds as follows. Generate $\eta_t \overset{i.i.d.}{\sim} \mathcal{N}(0,1)$ and compute a bootstrap residual $\boldsymbol{u}_t^* = \eta_t\hat{\boldsymbol{u}}_t$. Generate the bootstrap sample $\{\boldsymbol{y}_t^*\}_{t=1}^T$ according to the rule $\boldsymbol{y}_t^* = \hat{\boldsymbol{A}}_0 + \hat{\boldsymbol{A}}_1\boldsymbol{y}_{t-1}^* + \boldsymbol{u}_t^*$, where $\boldsymbol{y}_0^* = \boldsymbol{0}$ and the null hypothesis of non-causality is imposed. For example, when the null hypothesis of non-causality from y_1 to y_2 is considered, the $(2,1)$-element of $\hat{\boldsymbol{A}}_1$ is forced to be 0. Given $\{\boldsymbol{y}_t^*\}_{t=1}^T$, compute a bootstrap Wald test statistic $\hat{\mathcal{W}}^*$ in the same way as the actual statistic $\hat{\mathcal{W}}$. Repeat these steps J times, resulting in $\{\hat{\mathcal{W}}_j^*\}_{j=1}^J$. Compute the bootstrap p-value as $\hat{p}_J^* = J^{-1}\sum_{j=1}^J \mathbf{1}(\hat{\mathcal{W}}_j^* \geq \hat{\mathcal{W}})$, where $\mathbf{1}(A)$ is the indicator function which takes 1 if event A occurs and 0 otherwise. Reject H_0 at the $100\alpha\%$ level if $\hat{p}_J^* < \alpha$, where $\alpha \in (0,1)$ is a nominal size.

Impose Assumptions (A1)-(A6) of HH2009 to ensure the asymptotic validity of the wild bootstrap. These assumptions require that $\boldsymbol{u}_t$ should be α-mixing and a martingale difference sequence with finite fourth moment. Various forms of conditional heteroscedasticity are allowed under Assumptions (A1)-(A6), including stationary generalized autoregressive conditional heteroscedasticity (GARCH). Proposition 2 of HH2009 states that, under H_0, the wild bootstrap is asymptotically valid in the following sense:

$$\sup_{0<c<\infty}\left|\Pr^*(\hat{\mathcal{W}}^* \leq c) - \Pr(\hat{\mathcal{W}} \leq c)\right| \xrightarrow{p} 0 \quad \text{as} \quad T \to \infty,$$

where $\Pr^*$ denotes the bootstrap probability measure.

3.1.2 Empirical results and robustness check

Let us apply the proposed Granger causality tests to the J-REIT data analyzed in the main paper. The number of bootstrap iterations is $J = 5000$, and the nominal size is $\alpha = 0.10$. The resulting bootstrap p-values are reported in Panel A of Table 4. For the pre-crisis hotel sector, the null hypothesis of non-causality from the central J-REIT to the local J-REIT at $h = 1$ is rejected with the p-value being 0.091. For the post-crisis hotel sector, non-causality from the local J-REIT to the central J-REIT is rejected with the p-value being 0.018. For the other cases, the null hypothesis of non-causality cannot be rejected.

The mutual non-causality found in the office and residential sectors suggests that these markets are weak-form efficient at least in a reduced form. Judging from the significant IRFs at $h = 0$ reported in Section 4 of the main paper, the instantaneous causality within each day should exist. Further, the significant IRFs at $h = 1$ suggest that the shock identification via the Cholesky decomposition helps us find structural interdependence. The significant causality detected in the hotel sector suggests that there is a stronger degree of predictability compared with the office and residential sectors.

In Appendix of the main paper, we conducted the robustness check by adding an extra control variable w. The first candidate is the yield spread between 10-year and 2-year bonds of the Japanese government. Let $R_{10,t}$ be the 10-year bond yield on day $t \in \{1, \ldots, T\}$.

Similarly, let $R_{2,t}$ be the 2-year bond yield. The yield spread is defined as $W_{1t} = R_{10,t} - R_{2,t}$, and its first difference is given by $w_{1t} = \Delta W_{1t} = W_{1t} - W_{1,t-1}$. The second candidate is the Nikkei Stock Average Volatility Index. Let V_t be the value of the Nikkei Stock Average Volatility Index, then the log-series is given by $W_{2t} = \ln V_t$ and the log-difference series is $w_{2t} = \Delta W_{2t}$.

We add either w_1 or w_2 to (1) as the fourth variable, and fit model (3). We then apply the Granger causality tests of HH2009 as described in this section. The resulting bootstrap p-values are reported in Panels B-C of Table 4. The results are similar to the main results shown in Panel A, indicating the robustness to the addition of extra control variables.

3.2 Confidence intervals of impulse responses

In this section, the MBB-based confidence interval of IRF is described. We focus on model (3) to keep notation simple, although MBB works for any lag length $p \in \mathbb{N}$. Assume that $\mathrm{E}(\boldsymbol{u}_t) = \boldsymbol{0}$ and $\mathrm{E}(\boldsymbol{u}_t \boldsymbol{u}_t^\top) = \boldsymbol{\Sigma}$, a $K \times K$ positive-definite symmetric matrix. Define the Cholesky decomposition $\boldsymbol{\Sigma} = \boldsymbol{L}\boldsymbol{L}^\top$, where $\boldsymbol{L}$ is a $K \times K$ lower triangular matrix. Model (3) can be transformed to a vector moving average model of order ∞ with an orthogonalized shock:

$$\boldsymbol{y}_t = \boldsymbol{\mu} + \sum_{k=0}^{\infty} \boldsymbol{\Theta}_k \boldsymbol{v}_{t-k},$$

where $\boldsymbol{\mu} = (\boldsymbol{I}_K - \boldsymbol{A}_1)^{-1}\boldsymbol{A}_0$, $\boldsymbol{\Theta}_k = \boldsymbol{A}_1^k \boldsymbol{L}$, and $\boldsymbol{v}_t = \boldsymbol{L}^{-1}\boldsymbol{u}_t$; note that $\mathrm{E}(\boldsymbol{v}_t) = \boldsymbol{0}$ and $\mathrm{E}(\boldsymbol{v}_t \boldsymbol{v}_t^\top) = \boldsymbol{I}_K$ by construction. Write $\boldsymbol{\Theta}_h = [\theta_{ij,h}]_{i,j}$, then $\theta_{ij,h}$ represents the (structural) IRF of series i to a 1σ shock in series j at prediction horizon $h \geq 0$. As in Section 3.1 of this supplemental material, execute the least squares to get the estimator $(\hat{\boldsymbol{A}}_0, \hat{\boldsymbol{A}}_1)$, residual $\hat{\boldsymbol{u}}_t$, and estimated error covariance matrix $\hat{\boldsymbol{\Sigma}}$. Implement the Cholesky decomposition to get $\hat{\boldsymbol{\Sigma}} = \hat{\boldsymbol{L}}\hat{\boldsymbol{L}}^\top$. The point estimator of IRF can be computed as $\hat{\boldsymbol{\Theta}}_k = \hat{\boldsymbol{A}}_1^k \hat{\boldsymbol{L}}$ for $k \geq 0$. To simplify exposition, let $\hat{\theta}$ signify a generic element of $\hat{\boldsymbol{\Theta}}_k$.

BJT2016 proposed that the $100(1-\alpha)\%$ confidence interval for $\hat{\theta}$ should be constructed as follows, where $\alpha \in (0,1)$ is a nominal size.

Step 1 Choose a block length $\ell < T$ and let $N = \lceil T/\ell \rceil$ be the number of blocks so that $\ell N \geq T$. Define a $K \times \ell$ block $\boldsymbol{B}_{i,\ell} = (\hat{\boldsymbol{u}}_{i+1}, \dots, \hat{\boldsymbol{u}}_{i+\ell})$ for $i \in \{0, \dots, T-\ell\}$.

Step 2 Draw $(i_0, \dots, i_{N-1})$ independently and identically from $\{0, 1, \dots, T-\ell\}$ with uniform probability. Stack blocks $(\boldsymbol{B}_{i_0,\ell}, \dots, \boldsymbol{B}_{i_{N-1},\ell})$ horizontally, and discard the last $N\ell - T$ columns to get bootstrap residuals $(\hat{\boldsymbol{u}}_1^*, \ldots, \hat{\boldsymbol{u}}_T^*)$. Center the bootstrap residuals according to the rule $\boldsymbol{u}_{j\ell+s}^* = \hat{\boldsymbol{u}}_{j\ell+s}^* - (T - \ell + 1)^{-1} \sum_{k=0}^{T-\ell} \hat{\boldsymbol{u}}_{s+k}$ for $s \in \{1, \ldots, \ell\}$ and $j \in \{0, 1, \ldots, N-1\}$ to ensure $\mathrm{E}^*(\boldsymbol{u}_t^*) = \boldsymbol{0}$ for all $t \in \{1, \ldots, T\}$.

Step 3 Generate the bootstrap sample $(\boldsymbol{y}_1^*, \ldots, \boldsymbol{y}_T^*)$ according to the rule $\boldsymbol{y}_t^* = \hat{\boldsymbol{A}}_0 + \hat{\boldsymbol{A}}_1 \boldsymbol{y}_{t-1}^* + \boldsymbol{u}_t^*$, where $\boldsymbol{y}_0^* = \boldsymbol{0}$. Compute IRF $\hat{\theta}^*$ given the bootstrap sample, where the procedure is the same as in the actual sample.

Step 4 Repeat Steps 2-3 J times, resulting in $(\hat{\theta}_1^*, \ldots, \hat{\theta}_J^*)$. Sort to get $\hat{\theta}_{(1)}^* \leq \cdots \leq \hat{\theta}_{(J)}^*$. The $100(1-\alpha)\%$ confidence interval for $\hat{\theta}$ is constructed via Hall's percentile interval: $\widehat{CI}_\alpha = [\hat{\theta} - \hat{\theta}_{\{(1-\alpha/2)J\}}^*,\ \hat{\theta} - \hat{\theta}_{\{(\alpha/2)J\}}^*]$.

Some regularity conditions need to be imposed on $\boldsymbol{u}_t$ for the MBB-based confidence interval to attain the asymptotic validity. Impose Assumptions 2.1 and 4.1 of BJT2016, and assume further that $\ell \to \infty$ and $\ell^3/T \to 0$ as $T \to \infty$; the suggested choice of Jentsch and Lunsford (2019), $\ell = \lfloor \kappa T^{1/4} \rfloor$ with $\kappa = 5.03$, satisfies the latter condition. Assumptions 2.1 and 4.1 of BJT2016 allow for a variety of conditionally heteroscedastic errors such as GARCH with a finite eighth moment. Corollary 5.2 of BJT2016 states that, under these regularity conditions, the MBB-based confidence interval is asymptotically valid in the following sense:

$$\sup_{x \in \mathbb{R}} \left| \Pr^* \left\{ \sqrt{T} \left(\hat{\theta}^* - \hat{\theta} \right) \leq x \right\} - \Pr \left\{ \sqrt{T} \left(\hat{\theta} - \theta \right) \leq x \right\} \right| \xrightarrow{p} 0 \quad \text{as} \quad T \to \infty.$$

This equation implies that the 90% confidence interval, for example, contains a true IRF with probability approaching 0.9 as $T \to \infty$.

Table 1: Japanese REIT securities listed on the Tokyo Stock Exchange

ID	Code	Abbr.	Full corporate name	Specializing in:
#01	8951	NBF	Nippon Building Fund Inc.	office
#02	8952	JRE	Japan Real Estate Investment Corporation	office
#03	8953	JMF	Japan Retail Fund Investment Corporation	commercial
#04	8954	OJR	ORIX JREIT Inc.	n/a
#05	8955	JPR	Japan Prime Realty Investment Corporation	n/a
#06	8956	NUD	Premier Investment Corporation	n/a
#07	8957	TRE	TOKYU REIT, Inc.	n/a
#08	8958	GOR	Global One Real Estate Investment Corporation	office
#09	8960	UUR	United Urban Investment Corporation	n/a
#10	8961	MTR	MORI TRUST Sogo Reit, Inc.	n/a
#11	8964	FRI	Frontier Real Estate Investment Corporation	commercial
#12	8966	HFR	HEIWA REAL ESTATE REIT, Inc.	n/a
#13	8967	JLF	Japan Logistics Fund, Inc.	logistics
#14	8968	FRC	Fukuoka REIT Corporation	n/a
#15	8972	KDO	Kenedix Office Investment Corporation	office
#16	8975	IRE	Ichigo Office REIT Investment Corporation	office
#17	8976	DOI	Daiwa Office Investment Corporation	office
#18	8977	HRI	Hankyu Hanshin REIT, Inc.	n/a
#19	8984	DHR	Daiwa House REIT Investment Corporation	n/a
#20	8985	JHR	Japan Hotel REIT Investment Corporation	hotel
#21	8986	DLI	Daiwa Securities Living Investment Corporation	residential
#22	8987	JEI	Japan Excellent, Inc.	office
#23	8963	INV	Invincible Investment Corporation	hotel
#24	3226	NAF	Nippon Accommodations Fund Inc.	residential
#25	3227	MCU	MCUBS MidCity Investment Corporation	office
#26	3234	MHR	Mori Hills REIT Investment Corporation	office
#27	3249	IIF	Industrial & Infrastructure Fund Investment Corporation	n/a
#28	3269	ADR	Advance Residence Investment Corporation	residential
#29	8979	SPI	Starts Proceed Investment Corporation	residential
#30	3278	KDR	Kenedix Residential Next Investment Corporation	n/a
#31	3279	API	Activia Properties Inc.	n/a

This table shows all 62 J-REIT securities listed on TSE as of February 5, 2021. The securities are sorted in ascending order in terms of the TSE listing date. ID: The identification number assigned by the authors. Code: The trade code assigned by TSE. Abbr.: The abbreviation defined by Japan REIT DB. “Specialization” is defined as individual properties of a single type accounting for 80% or more of the total appraisal value of a portfolio. “n/a” means that the relevant J-REIT does not specialize in any property type.

Table 1: Japanese REIT securities listed on the Tokyo Stock Exchange (continued)

ID	Code	Abbr.	Full corporate name	Specializing in:
#32	3281	GLP	GLP J-REIT	logistics
#33	3282	CRR	Comforia Residential REIT, Inc	residential
#34	3283	NPR	Nippon Prologis REIT, Inc.	logistics
#35	3287	HRR	Hoshino Resorts REIT, Inc.	hotel
#36	3290	ORI	One REIT, Inc.	office
#37	3292	ARI	AEON REIT Investment Corporation	commercial
#38	3295	HLR	Hulic Reit, Inc.	n/a
#39	3296	NRIC	NIPPON REIT Investment Corporation	n/a
#40	3298	IOJ	Invesco Office J-REIT, Inc.	office
#41	3451	TRIC	Tosei Reit Investment Corporation	n/a
#42	3309	SHRI	Sekisui House Reit, Inc.	n/a
#43	3453	KRR	Kenedix Retail REIT Corporation	n/a
#44	3455	HCM	Healthcare & Medical Investment Corporation	others
#45	3459	SRIC	Samty Residential Investment Corporation	residential
#46	3462	NMF	Nomura Real Estate Master Fund, Inc.	n/a
#47	3463	IHR	Ichigo Hotel REIT Investment Corporation	hotel
#48	3466	LLR	LaSalle LOGIPORT REIT	logistics
#49	3468	SAIC	Star Asia Investment Corporation	n/a
#50	3470	MRR	marimo Regional Revitalization REIT, Inc.	n/a
#51	3471	MFLP	Mitsui Fudosan Logistics Park Inc.	logistics
#52	3472	OOR	Ooedo Onsen Reit Investment Corporation	hotel
#53	3476	MIR	MIRAI Corporation	n/a
#54	3478	MTH	MORI TRUST Hotel Reit, Inc.	hotel
#55	3481	MEL	Mitsubishi Estate Logistics REIT Investment Corporation	logistics
#56	3487	CRE	CRE Logistics REIT, Inc.	logistics
#57	3488	XRI	XYMAX REIT Investment Corporation	n/a
#58	3492	TLR	Takara Leben Real Estate Investment Corporation	n/a
#59	3493	IAL	ITOCHU Advance Logistics Investment Corporation	logistics
#60	2971	EJR	ESCON JAPAN REIT Investment Corporation	n/a
#61	2972	SRE	SANKEI REAL ESTATE Inc.	office
#62	2979	SLR	SOSiLA Logistics REIT, Inc.	logistics

This table shows all 62 J-REIT securities listed on TSE as of February 5, 2021. The securities are sorted in ascending order in terms of the TSE listing date. ID: The identification number assigned by the authors. Code: The trade code assigned by TSE. Abbr.: The abbreviation defined by Japan REIT DB. “Specialization” is defined as individual properties of a single type accounting for 80% or more of the total appraisal value of a portfolio. “n/a” means that the relevant J-REIT does not specialize in any property type.

Table 2: Regional decompositions of commercial and logistics J-REITs

Regional decompositions of commercial J-REITs (%)

ID	Code	Abbr.	Tokyo5	Tokyo23	TokyoP	Kanto	C&K	Others	(Commercial)
#03	8953	JMF	20.6	5.3	8.7	18.0	38.6	8.7	96.3
#11	8964	FRI	5.0	22.8	3.5	23.5	29.5	15.7	89.6
#37	3292	ARI	0.0	0.0	0.0	33.3	33.9	32.8	90.3

Regional decompositions of logistics J-REITs (%)

ID	Code	Abbr.	Tokyo5	Tokyo23	TokyoP	Kanto	C&K	Others	(Logistics)
#13	8967	JLF	0.0	13.7	10.3	57.3	16.2	2.5	100
#32	3281	GLP	0.0	17.2	2.7	39.6	29.0	11.5	100
#34	3283	NPR	0.0	7.2	0.0	52.9	37.0	3.0	100
#48	3466	LLR	0.0	0.0	0.0	76.1	23.9	0.0	97.3
#51	3471	MFLP	0.0	0.0	7.4	71.8	17.6	3.2	92.5
#55	3481	MEL	0.0	0.0	0.0	57.6	32.2	10.3	95.3
#56	3487	CRE	0.0	0.0	8.6	87.5	0.0	4.0	100
#59	3493	IAL	0.0	0.0	0.0	100	0.0	0.0	100
#62	2979	SLR	0.0	0.0	0.0	68.7	31.3	0.0	91.2

This table presents the regional decompositions of the commercial and logistics J-REITs based on the first financial statements of 2020. The sector-specific J-REIT is defined as a company whose individual properties of a given type account for 80% or more of the total appraisal value of the portfolio. ID: The identification number assigned by the authors in terms of the TSE listing date. Code: The trade code assigned by TSE. Abbr.: The abbreviation assigned by Japan REIT DB. Tokyo5: Central five wards of Tokyo. Tokyo23: The twenty-three wards of Tokyo excluding Tokyo5. TokyoP: Tokyo Prefecture excluding Tokyo23. Kanto: Kanto Area excluding TokyoP. C&K: Chubu and Kinki Areas. Others: Other regions not classified above.

Table 3: Sample statistics of the daily log-returns of all J-REIT shares in the crisis period (#01–#21)

ID	Abbr.	mean	median	min	max	stdev	skew	kurt
#01	NBF	−0.007	−0.006	−0.166	0.153	0.051	0.431	6.119
#02	JRE	−0.007	−0.002	−0.182	0.130	0.049	−0.284	6.389
#03	JMF	−0.015	−0.014	−0.268	0.232	0.078	−0.301	6.012
#04	OJR	−0.012	−0.001	−0.250	0.192	0.074	−0.176	5.769
#05	JPR	−0.011	−0.011	−0.264	0.185	0.072	−0.318	6.867
#06	NUD	−0.009	−0.007	−0.182	0.148	0.065	−0.169	3.980
#07	TRE	−0.008	−0.002	−0.251	0.157	0.073	−0.301	5.174
#08	GOR	−0.010	−0.010	−0.201	0.148	0.063	−0.235	4.647
#09	UUR	−0.012	0.002	−0.322	0.165	0.077	−1.318	8.036
#10	MTR	−0.011	−0.008	−0.154	0.169	0.053	0.311	5.449
#11	FRI	−0.008	−0.002	−0.146	0.130	0.050	−0.265	4.770
#12	HFR	−0.009	−0.007	−0.200	0.192	0.065	0.246	5.687
#13	JLF	−0.003	−0.005	−0.172	0.223	0.057	1.058	8.729
#14	FRC	−0.012	−0.005	−0.169	0.146	0.065	−0.316	3.951
#15	KDO	−0.011	−0.005	−0.147	0.165	0.060	0.161	3.778
#16	IRE	−0.012	−0.009	−0.169	0.150	0.059	−0.120	4.111
#17	DOI	−0.009	−0.013	−0.170	0.141	0.058	0.048	4.451
#18	HRI	−0.009	−0.008	−0.111	0.120	0.046	0.179	3.748
#19	DHR	−0.003	−0.002	−0.244	0.200	0.058	−0.585	10.56
#20	JHR	−0.014	−0.008	−0.232	0.164	0.080	−0.106	3.293
#21	DLI	−0.004	−0.002	−0.122	0.137	0.051	−0.016	4.331

Crisis period: February 27 – May 1, 2020 (45 days). ID: The identification number assigned by the authors in terms of the TSE listing date. Abbr.: The abbreviation assigned by Japan REIT DB. For each share, we report major sample statistics of the daily log-return: mean, median, minimum, maximum, standard deviation, skewness, and kurtosis. In this table, shares #01–#21 are covered.

Table 3: Sample statistics of the daily log-returns of all J-REIT shares in the crisis period (#22–#42)

ID	Abbr.	mean	median	min	max	stdev	skew	kurt
#22	JEI	−0.011	−0.007	−0.320	0.190	0.082	−0.572	7.116
#23	INV	−0.013	−0.013	−0.231	0.219	0.078	0.127	4.075
#24	NAF	−0.003	0.003	−0.204	0.147	0.054	−0.602	6.665
#25	MCU	−0.012	−0.006	−0.178	0.178	0.066	0.231	4.215
#26	MHR	−0.006	−0.006	−0.271	0.240	0.073	0.041	7.970
#27	IIF	−0.005	−0.005	−0.136	0.224	0.058	1.035	7.442
#28	ADR	−0.001	0.003	−0.214	0.214	0.064	−0.166	6.960
#29	SPI	−0.002	0.000	−0.078	0.093	0.036	0.017	3.417
#30	KDR	−0.004	−0.001	−0.176	0.200	0.061	0.282	6.005
#31	API	−0.013	−0.009	−0.250	0.153	0.063	−0.633	6.739
#32	GLP	−0.001	0.001	−0.171	0.171	0.062	0.355	4.945
#33	CRR	−0.002	0.000	−0.225	0.184	0.062	−0.148	7.412
#34	NPR	−0.001	−0.001	−0.204	0.204	0.052	0.060	10.81
#35	HRR	−0.008	−0.015	−0.130	0.145	0.059	0.397	3.208
#36	ORI	−0.010	−0.005	−0.194	0.163	0.059	−0.032	5.014
#37	ARI	−0.007	−0.003	−0.195	0.173	0.064	0.120	4.920
#38	HLR	−0.012	−0.010	−0.284	0.177	0.068	−0.715	8.314
#39	NRIC	−0.010	−0.009	−0.202	0.173	0.067	−0.084	4.835
#40	IOJ	−0.012	−0.009	−0.165	0.179	0.069	0.350	3.745
#41	TRIC	−0.007	−0.001	−0.183	0.103	0.055	−0.509	4.310
#42	SHRI	−0.007	−0.006	−0.184	0.159	0.058	0.057	5.511

Crisis period: February 27 – May 1, 2020 (45 days). ID: The identification number assigned by the authors in terms of the TSE listing date. Abbr.: The abbreviation assigned by Japan REIT DB. For each share, we report major sample statistics of the daily log-return: mean, median, minimum, maximum, standard deviation, skewness, and kurtosis. In this table, shares #22–#42 are covered. In the main analysis, #26 MHR is used as the central office J-REIT; #33 CRR is used as the central residential J-REIT; #36 ORI is used as the local office J-REIT.

Table 3: Sample statistics of the daily log-returns of all J-REIT shares in the crisis period (#43–#63)

ID	Abbr.	mean	median	min	max	stdev	skew	kurt
#43	KRR	−0.010	0.003	−0.239	0.187	0.075	−0.266	4.915
#44	HCM	−0.003	−0.001	−0.127	0.147	0.048	0.228	4.784
#45	SRIC	−0.002	0.005	−0.121	0.098	0.042	−0.384	3.907
#46	NMF	−0.010	−0.010	−0.323	0.221	0.081	−0.500	7.845
#47	IHR	−0.014	−0.010	−0.206	0.151	0.073	0.092	3.499
#48	LLR	−0.003	−0.005	−0.236	0.191	0.063	−0.131	7.501
#49	SAIC	−0.005	−0.004	−0.197	0.146	0.056	−0.269	5.878
#50	MRR	−0.006	−0.002	−0.183	0.125	0.054	−0.625	5.014
#51	MFLP	−0.004	−0.006	−0.189	0.189	0.056	−0.189	7.358
#52	OOR	−0.008	0.000	−0.142	0.101	0.053	−0.677	3.494
#53	MIR	−0.010	−0.003	−0.207	0.125	0.062	−0.568	4.408
#54	MTH	−0.011	−0.013	−0.154	0.129	0.061	0.144	3.721
#55	MEL	−0.004	−0.004	−0.121	0.124	0.046	0.191	4.352
#56	CRE	0.000	0.002	−0.154	0.163	0.058	0.022	4.453
#57	XRI	−0.009	−0.004	−0.153	0.107	0.051	−0.588	3.767
#58	TLR	−0.009	−0.001	−0.188	0.142	0.061	−0.191	4.017
#59	IAL	0.000	0.009	−0.155	0.187	0.056	−0.040	5.969
#60	EJR	−0.006	−0.002	−0.162	0.151	0.055	−0.254	4.428
#61	SRE	−0.008	0.002	−0.128	0.147	0.057	0.246	3.437
#62	SLR	−0.001	0.007	−0.166	0.120	0.047	−1.176	6.709
#63	TSE	−0.007	−0.007	−0.205	0.129	0.056	−0.388	6.283

Crisis period: February 27 – May 1, 2020 (45 days). ID: The identification number assigned by the authors in terms of the TSE listing date. Abbr.: The abbreviation assigned by Japan REIT DB. For each share, we report major sample statistics of the daily log-return: mean, median, minimum, maximum, standard deviation, skewness, and kurtosis. In this table, shares #43–#62 and #63 TSE REIT Index are covered. In the main analysis, #45 SRIC is used as the local residential J-REIT; #52 OOR is used as the local hotel J-REIT; #54 MTH is used as the central hotel J-REIT.

Table 4: Wild-bootstrap p-values of Granger causality tests

A. Trivariate scenario

	Pre-crisis period			Post-crisis period		
	Office	Residential	Hotel	Office	Residential	Hotel
$H_0 : y_1 \nrightarrow y_2$	0.633	0.805	0.091	0.983	0.152	0.919
$H_0 : y_2 \nrightarrow y_1$	0.368	0.297	0.298	0.349	0.263	0.018

B. Four-variable scenario with the yield spread

	Pre-crisis period			Post-crisis period		
	Office	Residential	Hotel	Office	Residential	Hotel
$H_0 : y_1 \nrightarrow y_2$	0.671	0.732	0.094	0.998	0.152	0.871
$H_0 : y_2 \nrightarrow y_1$	0.352	0.282	0.282	0.376	0.222	0.028

C. Four-variable scenario with the volatility index

	Pre-crisis period			Post-crisis period		
	Office	Residential	Hotel	Office	Residential	Hotel
$H_0 : y_1 \nrightarrow y_2$	0.633	0.856	0.111	0.933	0.090	0.814
$H_0 : y_2 \nrightarrow y_1$	0.361	0.319	0.256	0.376	0.386	0.024

(y_1, y_2) signify the log-returns of the central and local J-REITs, respectively. The central J-REIT means #26 MHR, #33 CRR, and #54 MTH for the office, residential, and hotel sectors, respectively. Similarly, the local J-REIT means #36 ORI, #45 SRIC, and #52 OOR. Model: $\boldsymbol{y}_t = \boldsymbol{A}_0 + \boldsymbol{A}_1 \boldsymbol{y}_{t-1} + \boldsymbol{u}_t$. Panel A: $\boldsymbol{y}_t = (y_{1t}, y_{2t}, z_t)^\top$, where z is the log-return of the TSE REIT Index. Panel B: $\boldsymbol{y}_t = (y_{1t}, y_{2t}, z_t, w_{1t})^\top$, where w_1 is the difference in the yield spread between 10-year and 2-year bonds of the Japanese government. Panel C: $\boldsymbol{y}_t = (y_{1t}, y_{2t}, z_t, w_{2t})^\top$, where w_2 is the log-difference of the Nikkei Stock Average Volatility Index. Pre-crisis period: February 7, 2017 – February 26, 2020 ($T = 745$ days). Post-crisis period: May 7, 2020 – March 11, 2022 ($T = 454$ days). We perform Granger causality tests assisted by the wild bootstrap of Hafner and Herwartz (2009), where the number of bootstrap iterations is $J = 5000$. This table reports the bootstrap p-values with respect to $H_0 : y_1 \nrightarrow y_2$ (i.e., Granger non-causality from y_1 to y_2 at horizon $h = 1$) and vice versa.

Figure 1: Daily stock prices and returns of J-REITs

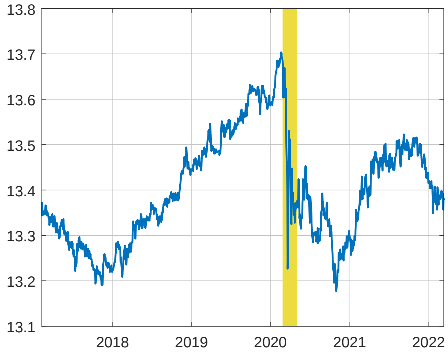

$\ln P_t$ (#01 NBF)

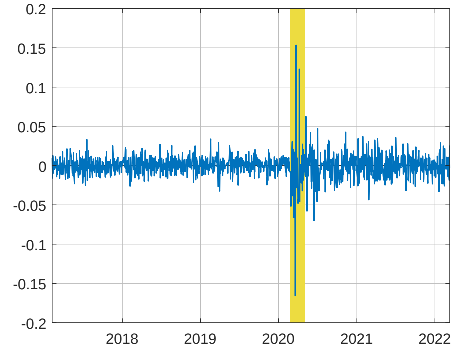

$\Delta \ln P_t$ (#01 NBF)

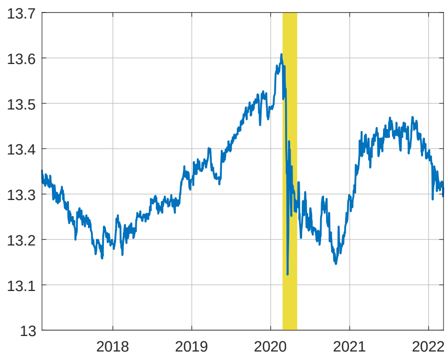

$\ln P_t$ (#02 JRE)

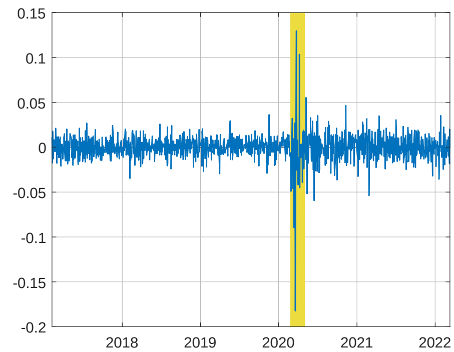

$\Delta \ln P_t$ (#02 JRE)

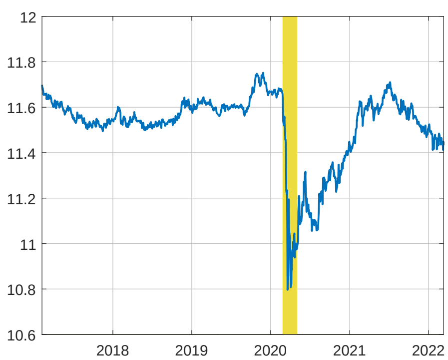

$\ln P_t$ (#03 JMF)

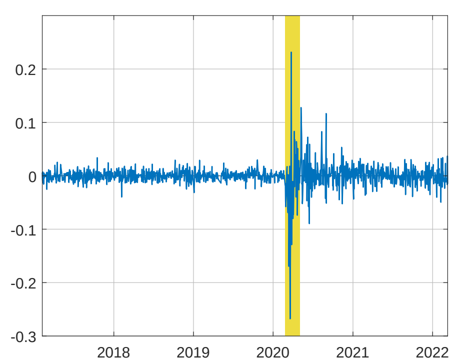

$\Delta \ln P_t$ (#03 JMF)

This figure plots the log-price $\ln P_t$ and the log-return $\Delta \ln P_t$ of individual J-REITs (#01–#03) from February 7, 2017 – March 11, 2022. The shaded area depicts the COVID-19 crisis period: February 27 – May 1, 2020.

Figure 1: Daily stock prices and returns of J-REITs (continued)

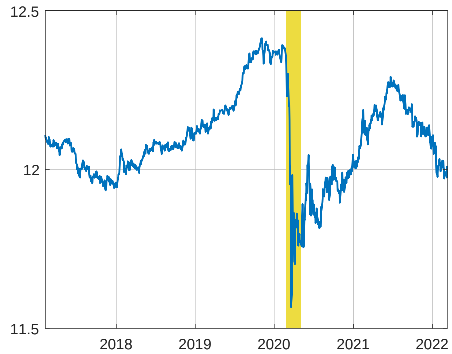

$\ln P_t$ (#04 OJR)

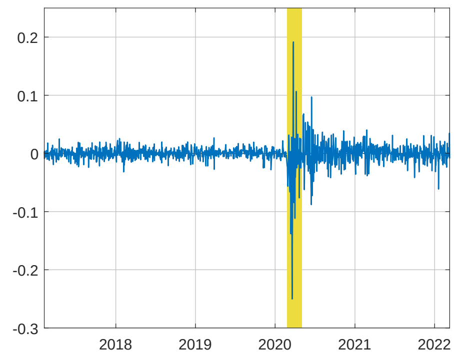

$\Delta \ln P_t$ (#04 OJR)

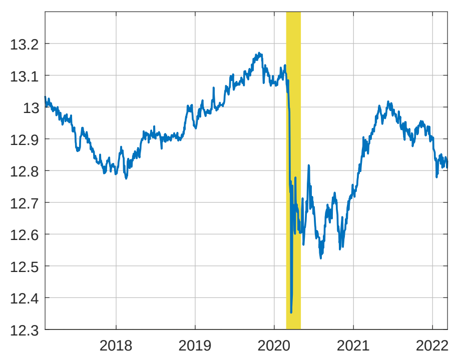

$\ln P_t$ (#05 JPR)

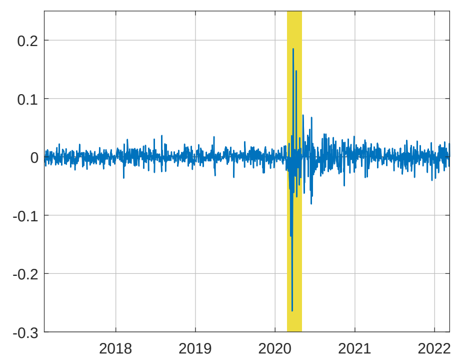

$\Delta \ln P_t$ (#05 JPR)

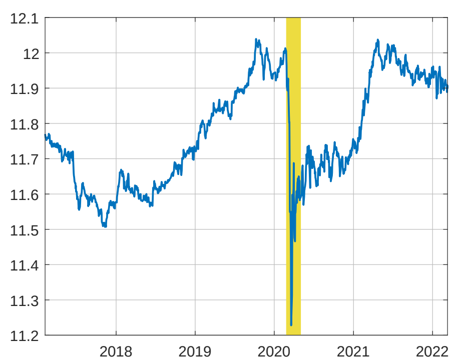

$\ln P_t$ (#06 NUD)

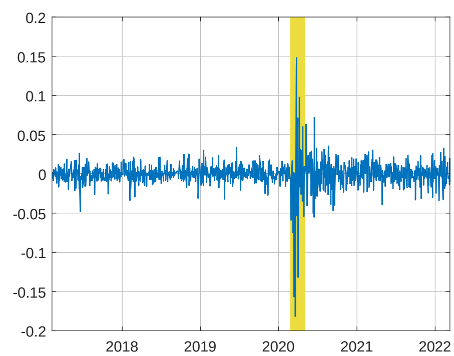

$\Delta \ln P_t$ (#06 NUD)

This figure plots the log-price $\ln P_t$ and the log-return $\Delta \ln P_t$ of individual J-REITs (#04–#06) from February 7, 2017 – March 11, 2022. The shaded area depicts the COVID-19 crisis period: February 27 – May 1, 2020.

Figure 1: Daily stock prices and returns of J-REITs (continued)

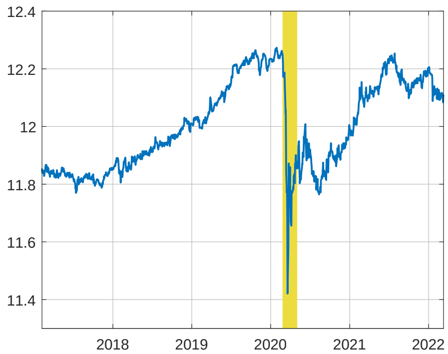

$\ln P_t$ (#07 TRE)

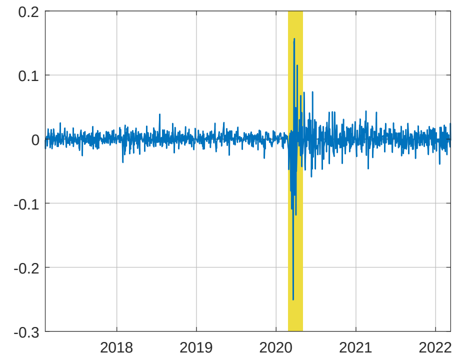

$\Delta \ln P_t$ (#07 TRE)

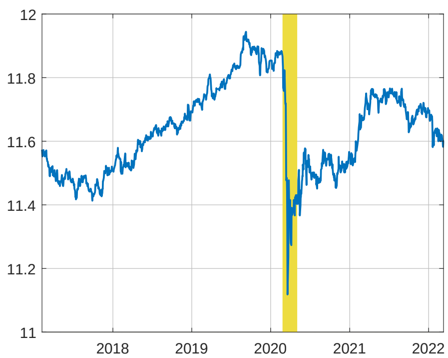

$\ln P_t$ (#08 GOR)

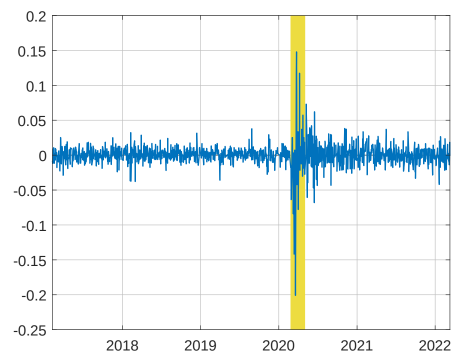

$\Delta \ln P_t$ (#08 GOR)

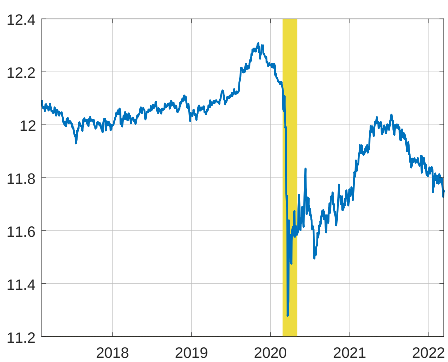

$\ln P_t$ (#09 UUR)

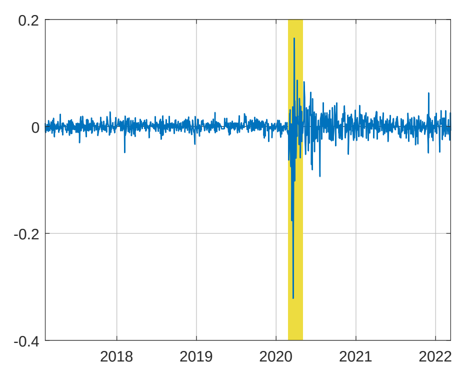

$\Delta \ln P_t$ (#09 UUR)

This figure plots the log-price $\ln P_t$ and the log-return $\Delta \ln P_t$ of individual J-REITs (#07–#09) from February 7, 2017 – March 11, 2022. The shaded area depicts the COVID-19 crisis period: February 27 – May 1, 2020.

Figure 1: Daily stock prices and returns of J-REITs (continued)

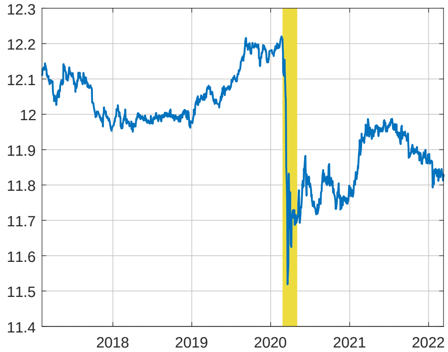

$\ln P_t$ (#10 MTR)

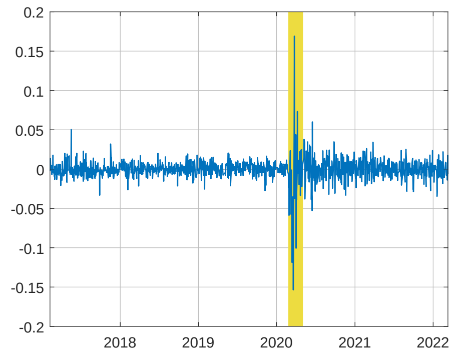

$\Delta \ln P_t$ (#10 MTR)

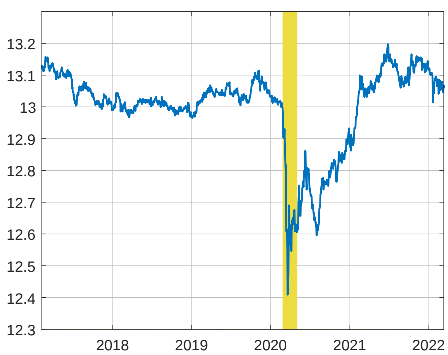

$\ln P_t$ (#11 FRI)

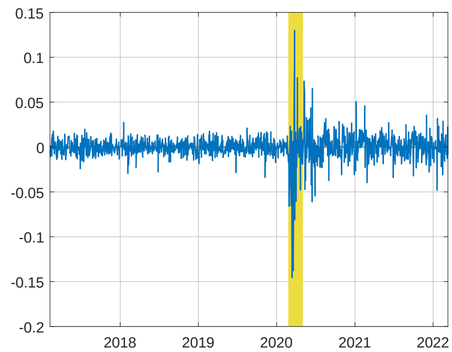

$\Delta \ln P_t$ (#11 FRI)

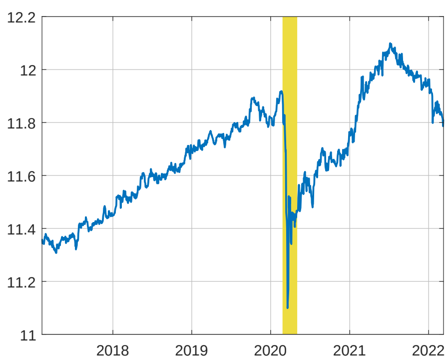

$\ln P_t$ (#12 HFR)

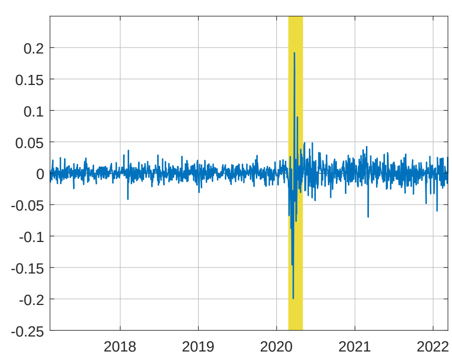

$\Delta \ln P_t$ (#12 HFR)

This figure plots the log-price $\ln P_t$ and the log-return $\Delta \ln P_t$ of individual J-REITs (#10–#12) from February 7, 2017 – March 11, 2022. The shaded area depicts the COVID-19 crisis period: February 27 – May 1, 2020.

Figure 1: Daily stock prices and returns of J-REITs (continued)

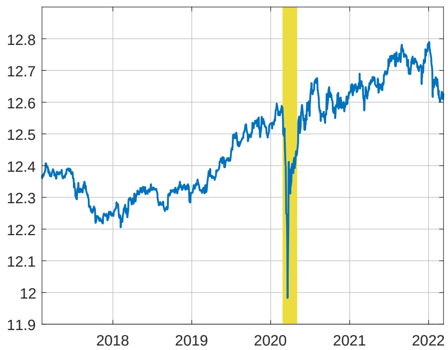

$\ln P_t$ (#13 JLF)

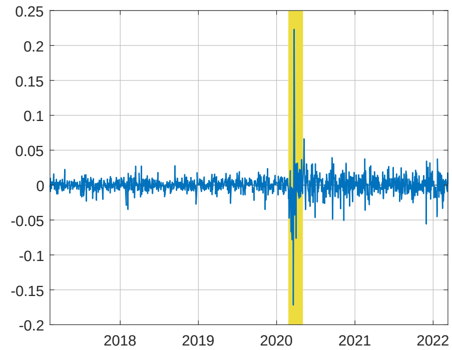

$\Delta \ln P_t$ (#13 JLF)

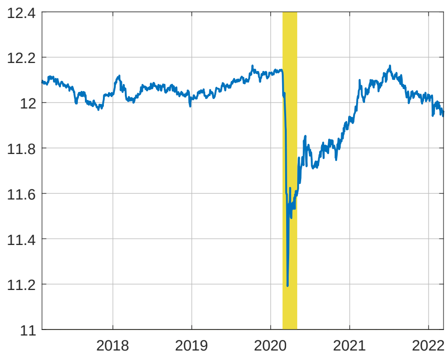

$\ln P_t$ (#14 FRC)

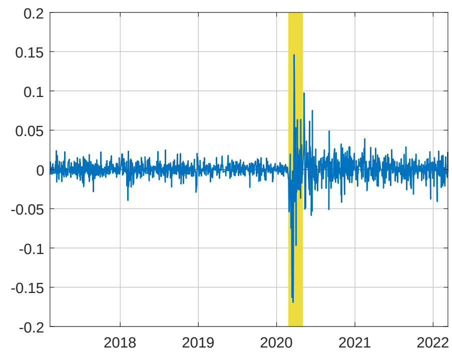

$\Delta \ln P_t$ (#14 FRC)

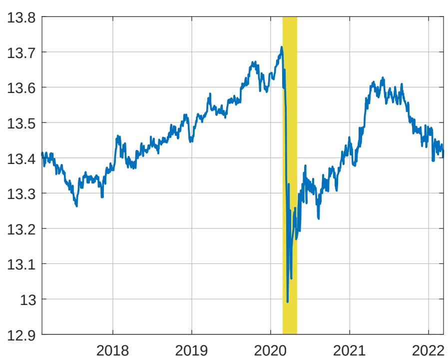

$\ln P_t$ (#15 KDO)

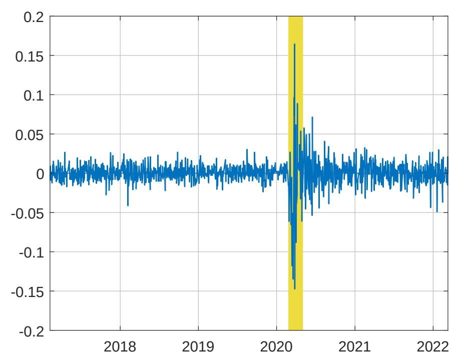

$\Delta \ln P_t$ (#15 KDO)

This figure plots the log-price $\ln P_t$ and the log-return $\Delta \ln P_t$ of individual J-REITs (#13–#15) from February 7, 2017 – March 11, 2022. The shaded area depicts the COVID-19 crisis period: February 27 – May 1, 2020.

Figure 1: Daily stock prices and returns of J-REITs (continued)

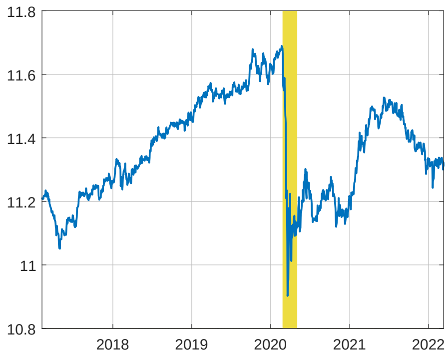

$\ln P_t$ (#16 IRE)

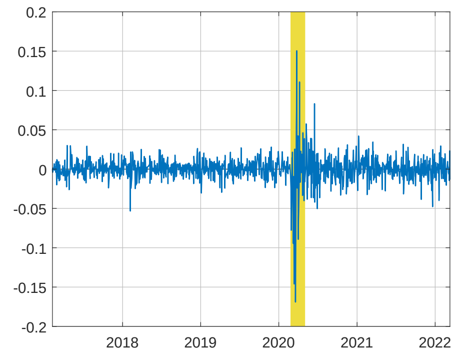

$\Delta \ln P_t$ (#16 IRE)

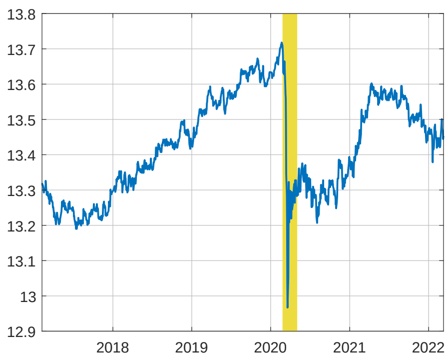

$\ln P_t$ (#17 DOI)

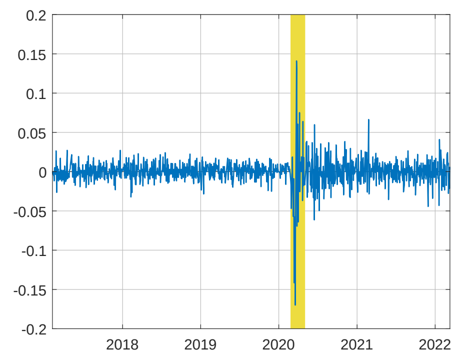

$\Delta \ln P_t$ (#17 DOI)

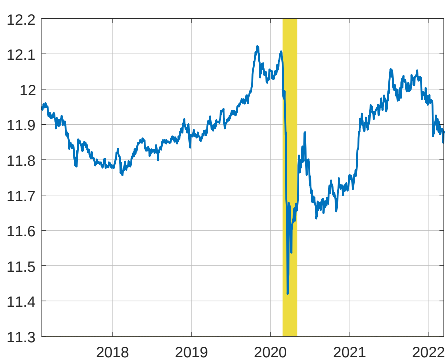

$\ln P_t$ (#18 HRI)

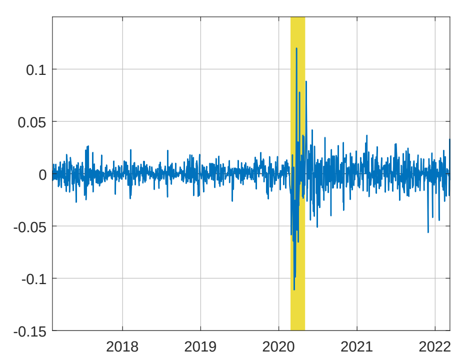

$\Delta \ln P_t$ (#18 HRI)

This figure plots the log-price $\ln P_t$ and the log-return $\Delta \ln P_t$ of individual J-REITs (#16–#18) from February 7, 2017 – March 11, 2022. The shaded area depicts the COVID-19 crisis period: February 27 – May 1, 2020.

Figure 1: Daily stock prices and returns of J-REITs (continued)

$\ln P_t$ (#19 DHR)

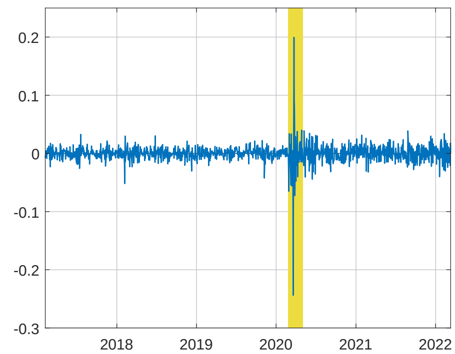

$\Delta \ln P_t$ (#19 DHR)

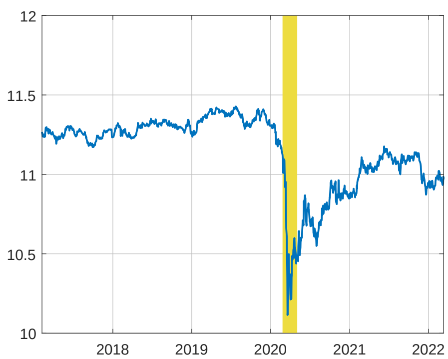

$\ln P_t$ (#20 JHR)

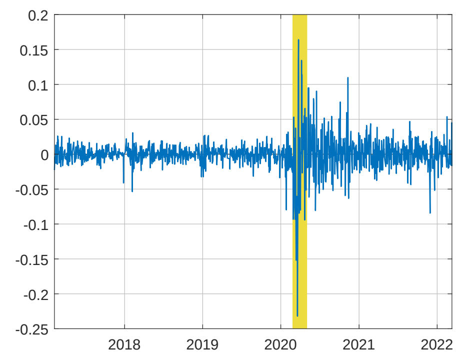

$\Delta \ln P_t$ (#20 JHR)

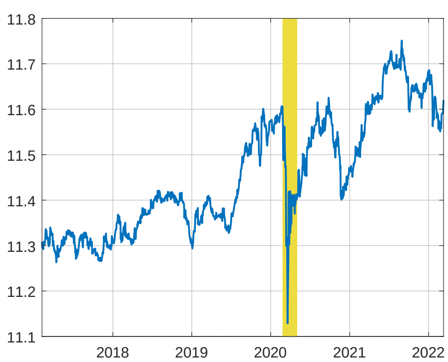

$\ln P_t$ (#21 DLI)

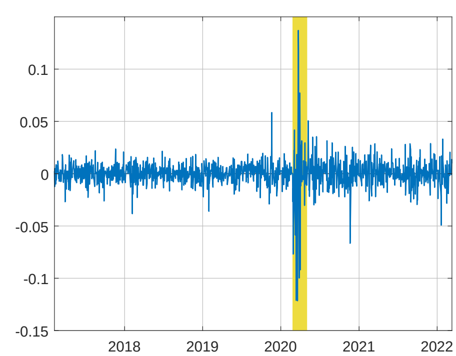

$\Delta \ln P_t$ (#21 DLI)

This figure plots the log-price $\ln P_t$ and the log-return $\Delta \ln P_t$ of individual J-REITs (#19–#21) from February 7, 2017 – March 11, 2022. The shaded area depicts the COVID-19 crisis period: February 27 – May 1, 2020.

Figure 1: Daily stock prices and returns of J-REITs (continued)

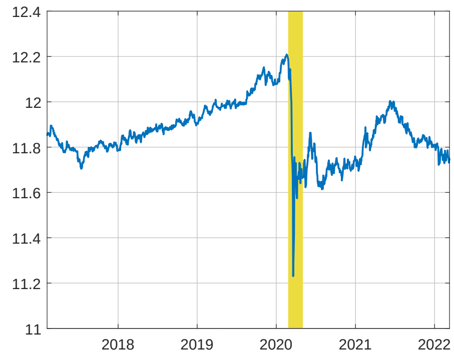

$\ln P_t$ (#22 JEI)

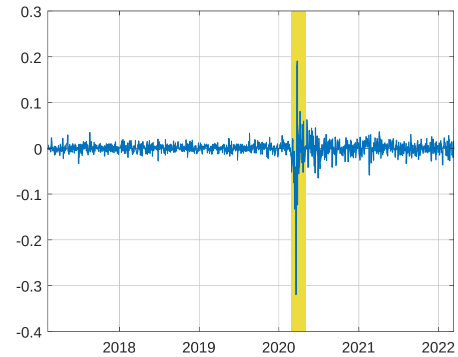

$\Delta \ln P_t$ (#22 JEI)

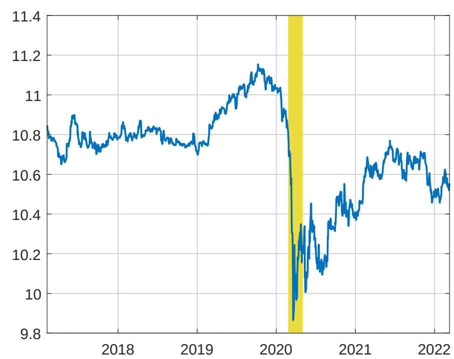

$\ln P_t$ (#23 INV)

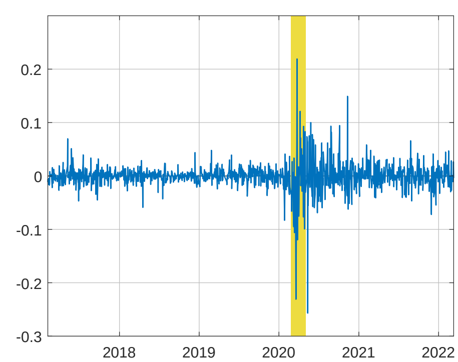

$\Delta \ln P_t$ (#23 INV)

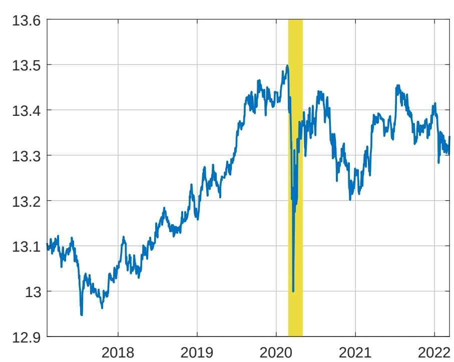

$\ln P_t$ (#24 NAF)

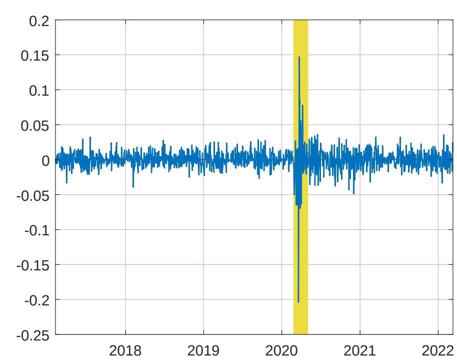

$\Delta \ln P_t$ (#24 NAF)

This figure plots the log-price $\ln P_t$ and the log-return $\Delta \ln P_t$ of individual J-REITs (#22–#24) from February 7, 2017 – March 11, 2022. The shaded area depicts the COVID-19 crisis period: February 27 – May 1, 2020.

Figure 1: Daily stock prices and returns of J-REITs (continued)

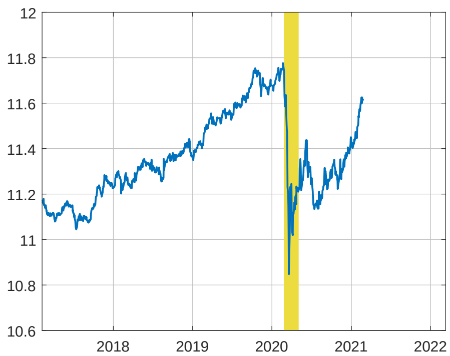

$\ln P_t$ (#25 MCU)

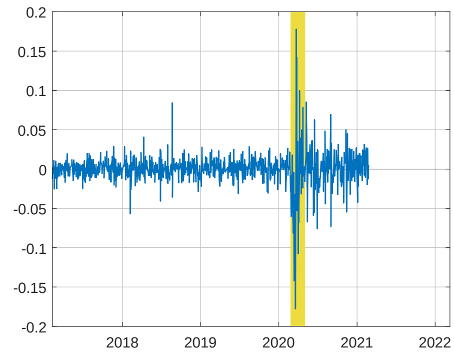

$\Delta \ln P_t$ (#25 MCU)

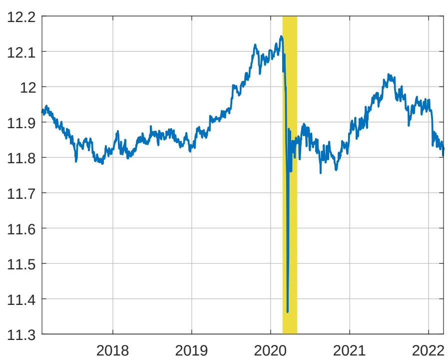

$\ln P_t$ (#26 MHR)

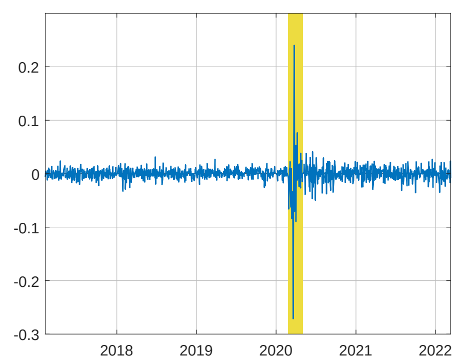

$\Delta \ln P_t$ (#26 MHR)

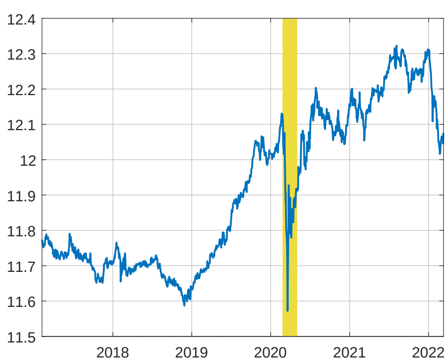

$\ln P_t$ (#27 IIF)

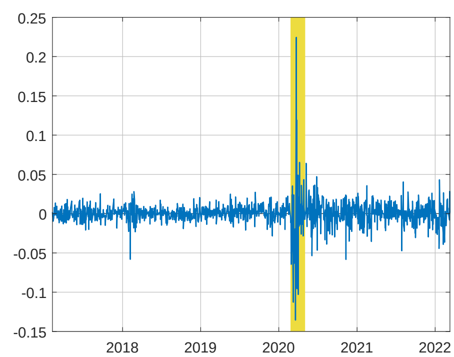

$\Delta \ln P_t$ (#27 IIF)

This figure plots the log-price $\ln P_t$ and the log-return $\Delta \ln P_t$ of individual J-REITs (#25–#27) from February 7, 2017 – March 11, 2022. The shaded area depicts the COVID-19 crisis period: February 27 – May 1, 2020. #25 MCU stopped being traded on February 24, 2021. In the main analysis, #26 MHR is chosen as the central office J-REIT.

Figure 1: Daily stock prices and returns of J-REITs (continued)

$\ln P_t$ (#28 ADR)

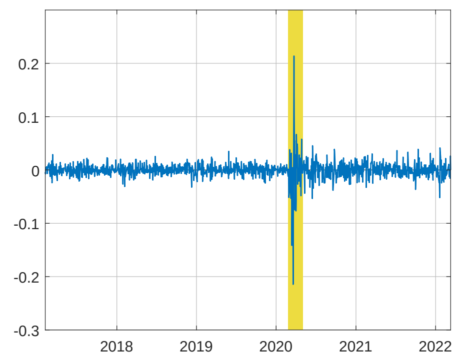

$\Delta \ln P_t$ (#28 ADR)

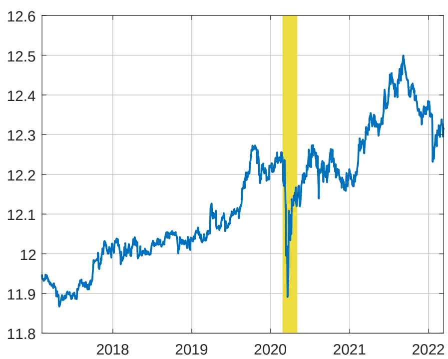

$\ln P_t$ (#29 SPI)

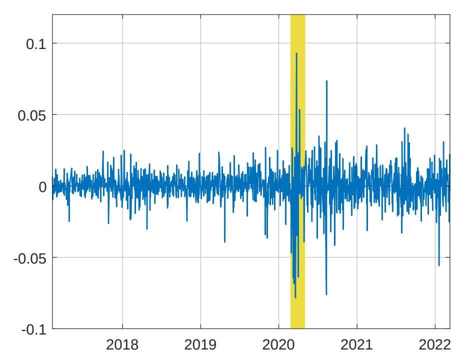

$\Delta \ln P_t$ (#29 SPI)

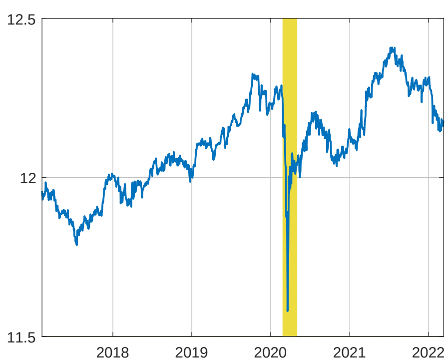

$\ln P_t$ (#30 KDR)

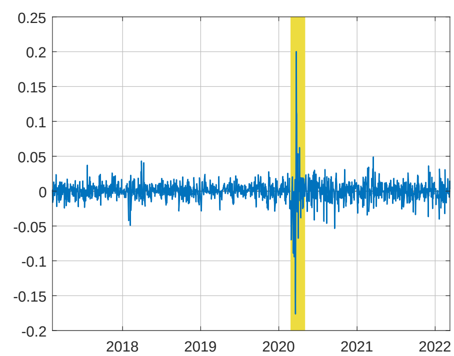

$\Delta \ln P_t$ (#30 KDR)

This figure plots the log-price $\ln P_t$ and the log-return $\Delta \ln P_t$ of individual J-REITs (#28–#30) from February 7, 2017 – March 11, 2022. The shaded area depicts the COVID-19 crisis period: February 27 – May 1, 2020.

Figure 1: Daily stock prices and returns of J-REITs (continued)

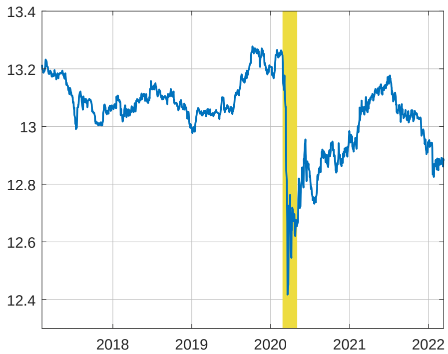

$\ln P_t$ (#31 API)

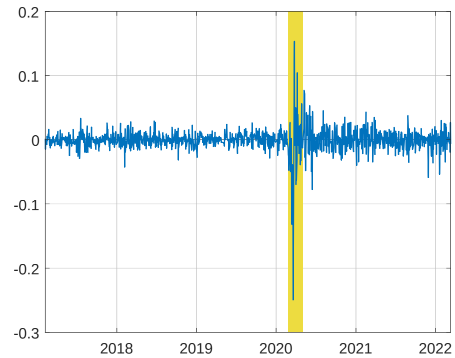

$\Delta \ln P_t$ (#31 API)

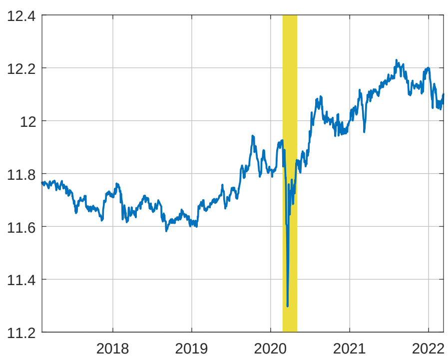

$\ln P_t$ (#32 GLP)

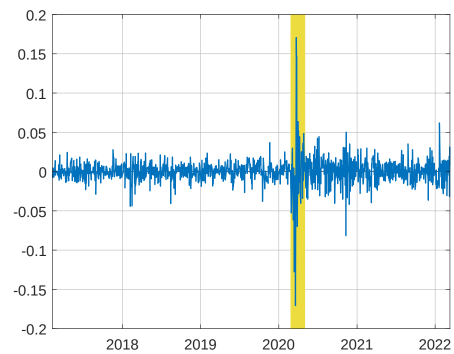

$\Delta \ln P_t$ (#32 GLP)

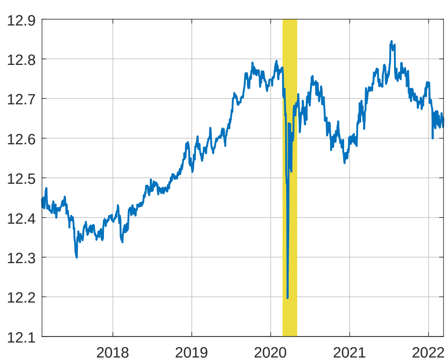

$\ln P_t$ (#33 CRR)

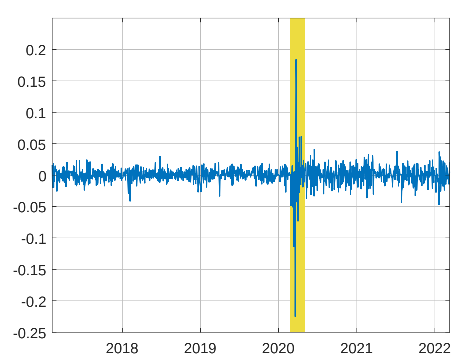

$\Delta \ln P_t$ (#33 CRR)

This figure plots the log-price $\ln P_t$ and the log-return $\Delta \ln P_t$ of individual J-REITs (#31–#33) from February 7, 2017 – March 11, 2022. The shaded area depicts the COVID-19 crisis period: February 27 – May 1, 2020. In the main analysis, #33 CRR is chosen as the central residential J-REIT.

Figure 1: Daily stock prices and returns of J-REITs (continued)

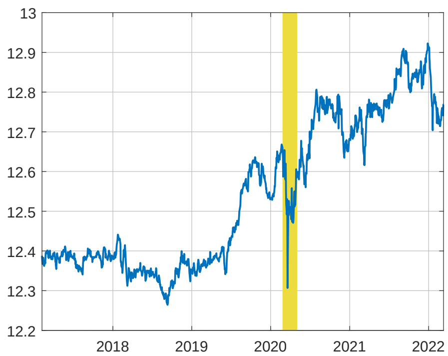

$\ln P_t$ (#34 NPR)

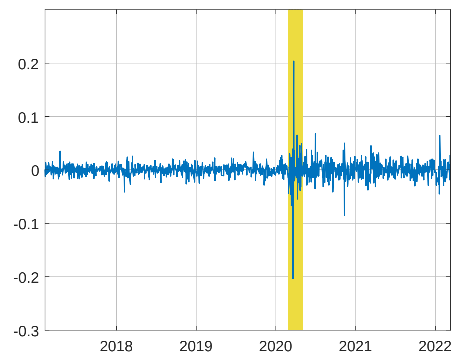

$\Delta \ln P_t$ (#34 NPR)

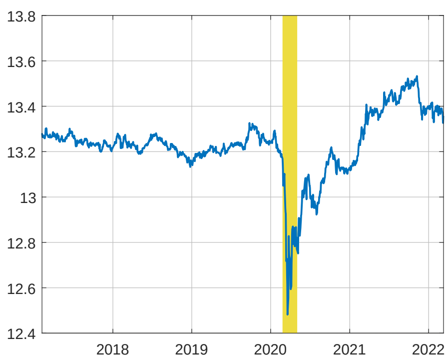

$\ln P_t$ (#35 HRR)

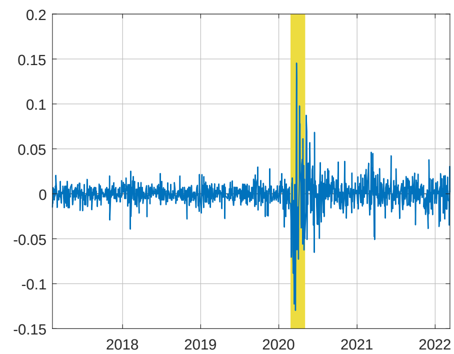

$\Delta \ln P_t$ (#35 HRR)

$\ln P_t$ (#36 ORI)

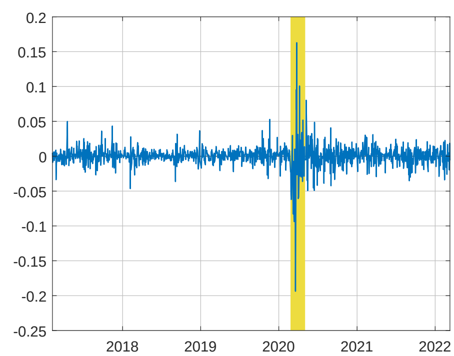

$\Delta \ln P_t$ (#36 ORI)

This figure plots the log-price $\ln P_t$ and the log-return $\Delta \ln P_t$ of individual J-REITs (#34–#36) from February 7, 2017 – March 11, 2022. The shaded area depicts the COVID-19 crisis period: February 27 – May 1, 2020. In the main analysis, #36 ORI is chosen as the local office J-REIT.

Figure 1: Daily stock prices and returns of J-REITs (continued)

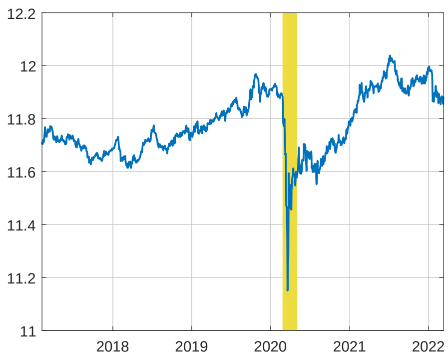

$\ln P_t$ (#37 ARI)

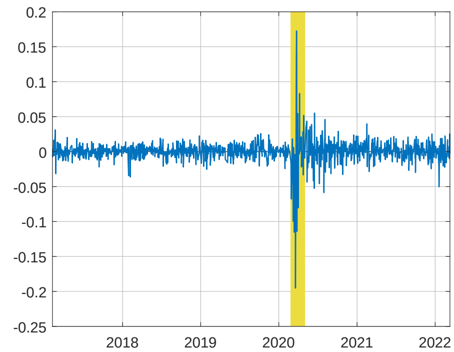

$\Delta \ln P_t$ (#37 ARI)

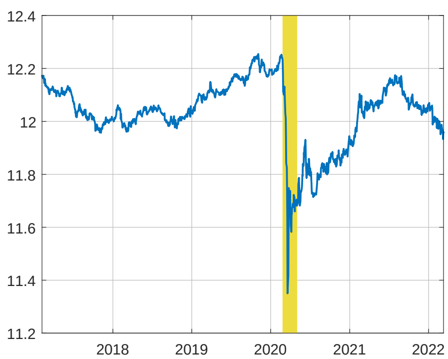

$\ln P_t$ (#38 HLR)

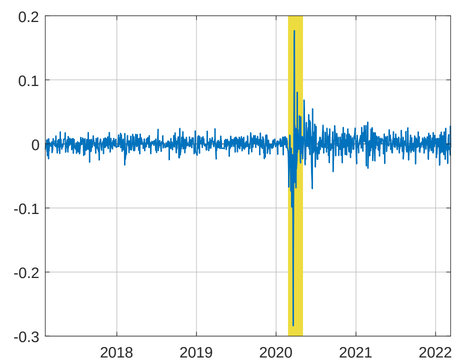

$\Delta \ln P_t$ (#38 HLR)

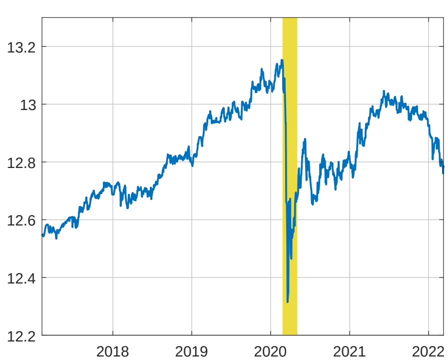

$\ln P_t$ (#39 NRIC)

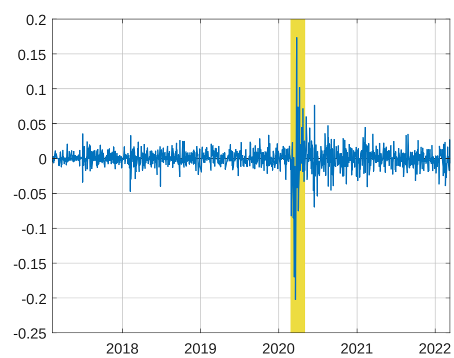

$\Delta \ln P_t$ (#39 NRIC)

This figure plots the log-price $\ln P_t$ and the log-return $\Delta \ln P_t$ of individual J-REITs (#37–#39) from February 7, 2017 – March 11, 2022. The shaded area depicts the COVID-19 crisis period: February 27 – May 1, 2020.

Figure 1: Daily stock prices and returns of J-REITs (continued)

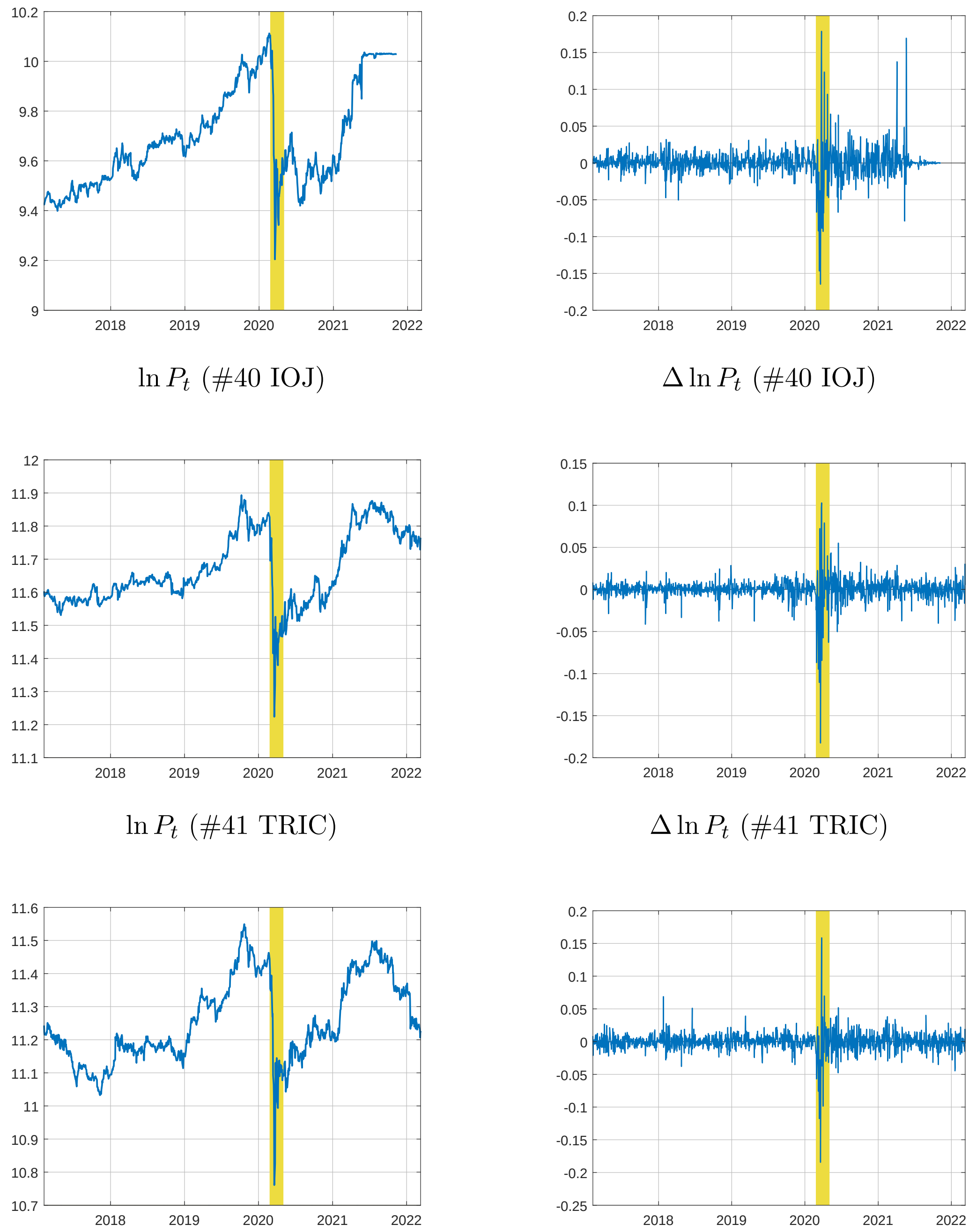

$\ln P_t$ (#40 IOJ) $\Delta \ln P_t$ (#40 IOJ)

$\ln P_t$ (#41 TRIC) $\Delta \ln P_t$ (#41 TRIC)

$\ln P_t$ (#42 SHRI) $\Delta \ln P_t$ (#42 SHRI)

This figure plots the log-price $\ln P_t$ and the log-return $\Delta \ln P_t$ of individual J-REITs (#40–#42) from February 7, 2017 – March 11, 2022. The shaded area depicts the COVID-19 crisis period: February 27 – May 1, 2020. #40 IOJ stopped being traded on November 8, 2021.

Figure 1: Daily stock prices and returns of J-REITs (continued)

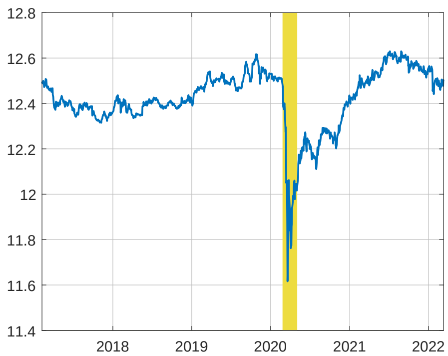

$\ln P_t$ (#43 KRR)

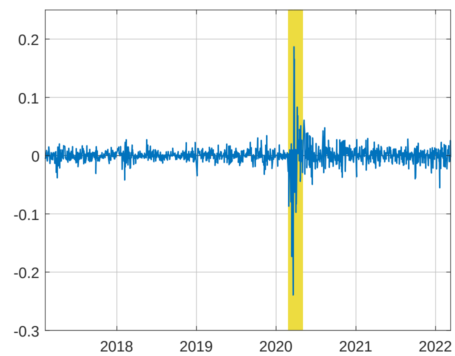

$\Delta \ln P_t$ (#43 KRR)

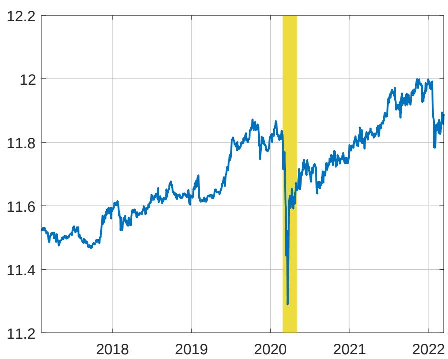

$\ln P_t$ (#44 HCM)

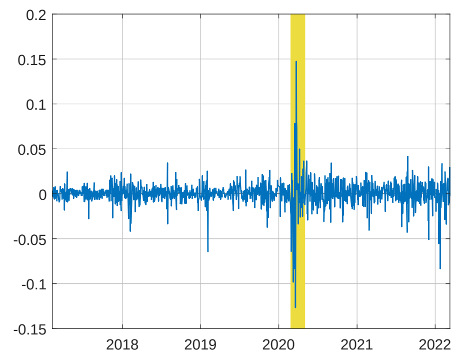

$\Delta \ln P_t$ (#44 HCM)

$\ln P_t$ (#45 SRIC)

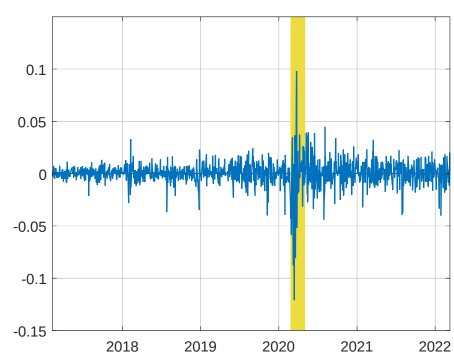

$\Delta \ln P_t$ (#45 SRIC)

This figure plots the log-price $\ln P_t$ and the log-return $\Delta \ln P_t$ of individual J-REITs (#43–#45) from February 7, 2017 – March 11, 2022. The shaded area depicts the COVID-19 crisis period: February 27 – May 1, 2020. In the main analysis, #45 SRIC is chosen as the local residential J-REIT.

Figure 1: Daily stock prices and returns of J-REITs (continued)

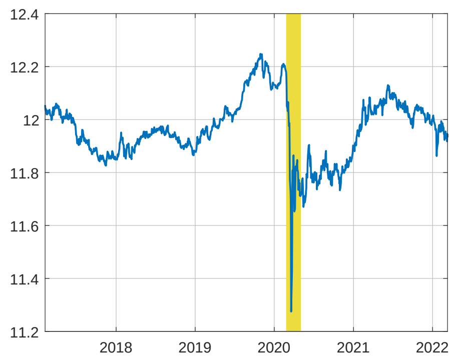

$\ln P_t$ (#46 NMF)

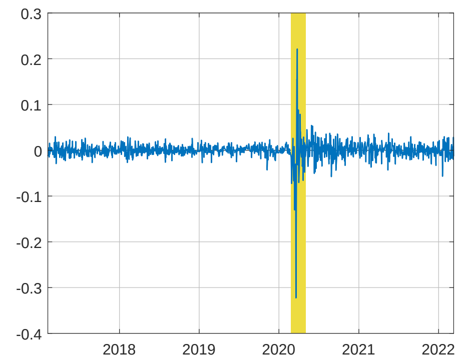

$\Delta \ln P_t$ (#46 NMF)

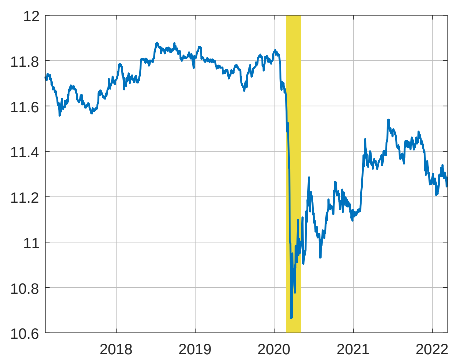

$\ln P_t$ (#47 IHR)

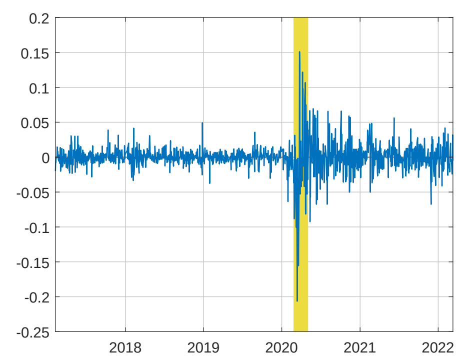

$\Delta \ln P_t$ (#47 IHR)

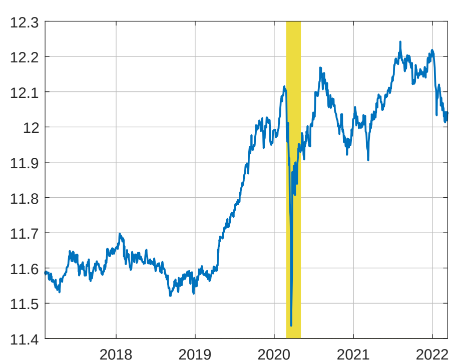

$\ln P_t$ (#48 LLR)

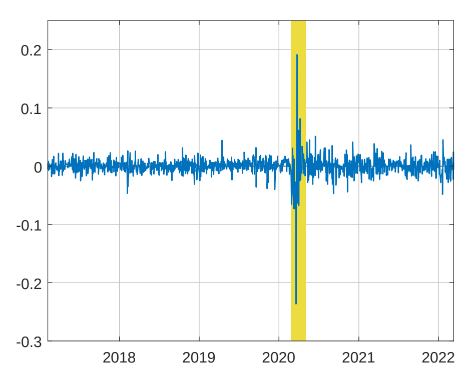

$\Delta \ln P_t$ (#48 LLR)

This figure plots the log-price $\ln P_t$ and the log-return $\Delta \ln P_t$ of individual J-REITs (#46–#48) from February 7, 2017 – March 11, 2022. The shaded area depicts the COVID-19 crisis period: February 27 – May 1, 2020.

Figure 1: Daily stock prices and returns of J-REITs (continued)

$\ln P_t$ (#49 SAIC)

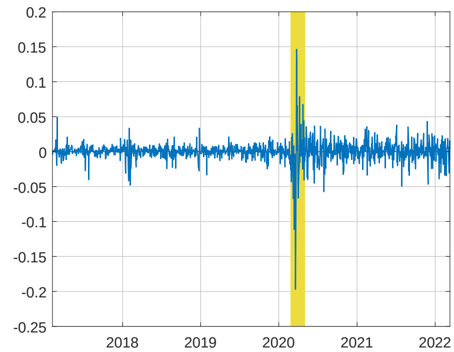

$\Delta \ln P_t$ (#49 SAIC)

$\ln P_t$ (#50 MRR)

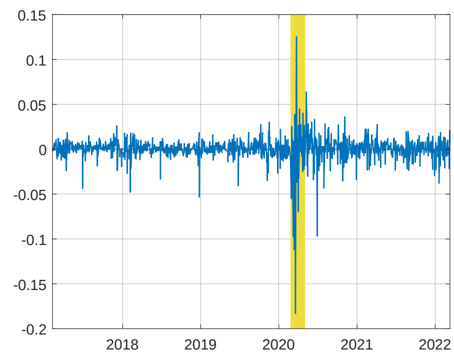

$\Delta \ln P_t$ (#50 MRR)

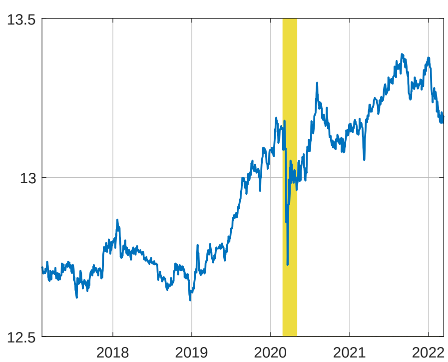

$\ln P_t$ (#51 MFLP)

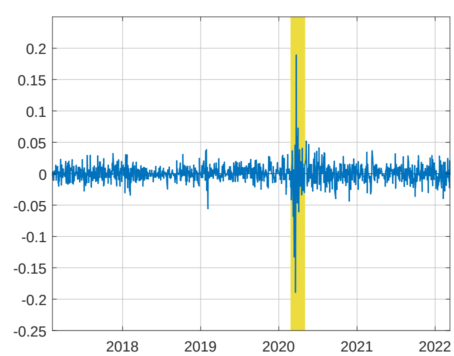

$\Delta \ln P_t$ (#51 MFLP)

This figure plots the log-price $\ln P_t$ and the log-return $\Delta \ln P_t$ of individual J-REITs (#49–#51) from February 7, 2017 – March 11, 2022. The shaded area depicts the COVID-19 crisis period: February 27 – May 1, 2020.

Figure 1: Daily stock prices and returns of J-REITs (continued)

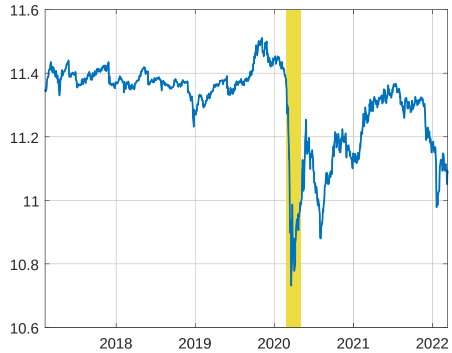

$\ln P_t$ (#52 OOR)

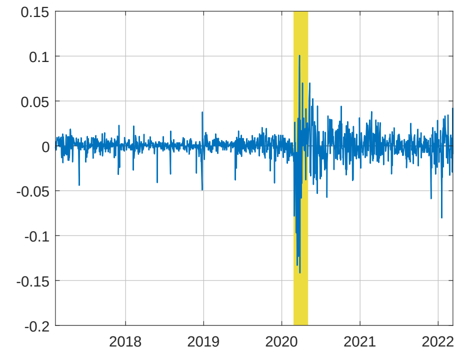

$\Delta \ln P_t$ (#52 OOR)

$\ln P_t$ (#53 MIR)

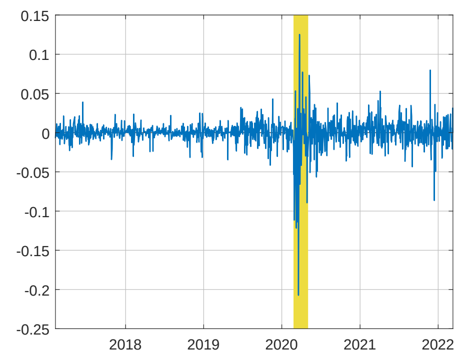

$\Delta \ln P_t$ (#53 MIR)

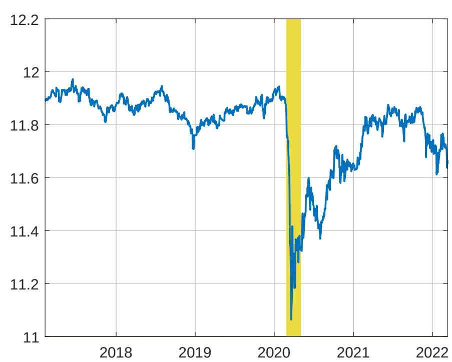

$\ln P_t$ (#54 MTH)

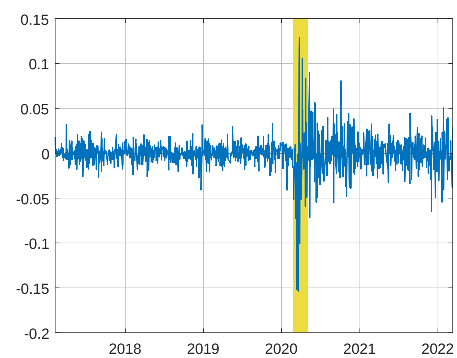

$\Delta \ln P_t$ (#54 MTH)

This figure plots the log-price $\ln P_t$ and the log-return $\Delta \ln P_t$ of individual J-REITs (#52–#54) from February 7, 2017 – March 11, 2022. The shaded area depicts the COVID-19 crisis period: February 27 – May 1, 2020. In the main analysis, #52 OOR is chosen as the local hotel J-REIT, and #54 MTH is chosen as the central hotel J-REIT.

Figure 1: Daily stock prices and returns of J-REITs (continued)

$\ln P_t$ (#55 MEL)

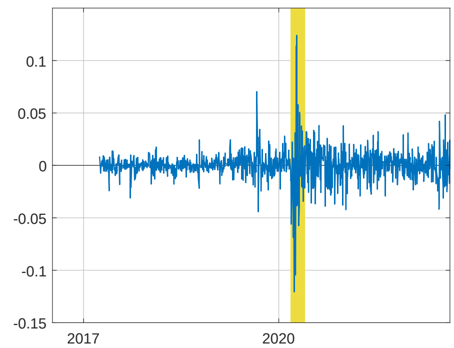

$\Delta \ln P_t$ (#55 MEL)

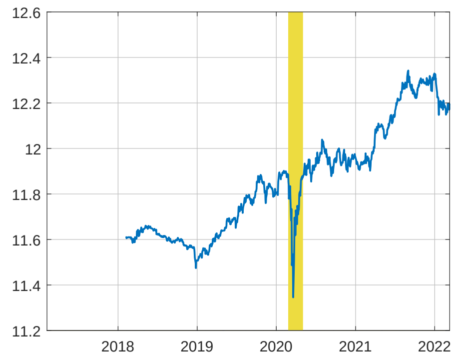

$\ln P_t$ (#56 CRE)

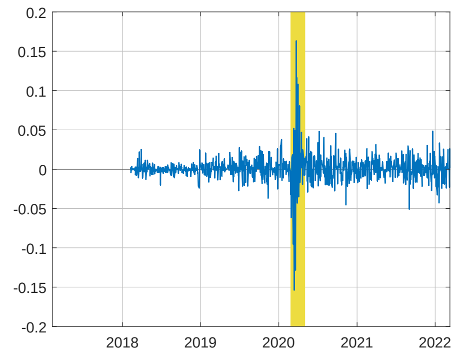

$\Delta \ln P_t$ (#56 CRE)

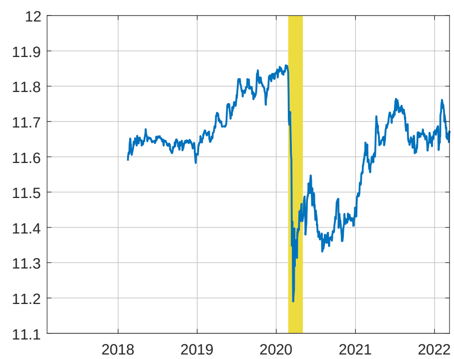

$\ln P_t$ (#57 XRI)

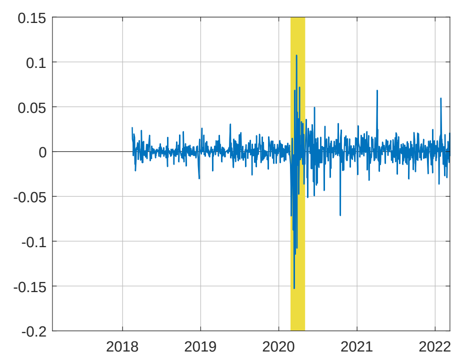

$\Delta \ln P_t$ (#57 XRI)

This figure plots the log-price $\ln P_t$ and the log-return $\Delta \ln P_t$ of individual J-REITs (#55–#57) from February 7, 2017 – March 11, 2022. The shaded area depicts the COVID-19 crisis period: February 27 – May 1, 2020. #55 MEL began being traded on September 15, 2017. #56 CRE began being traded on February 7, 2018. #57 XRI began being traded on February 15, 2018.

Figure 1: Daily stock prices and returns of J-REITs (continued)

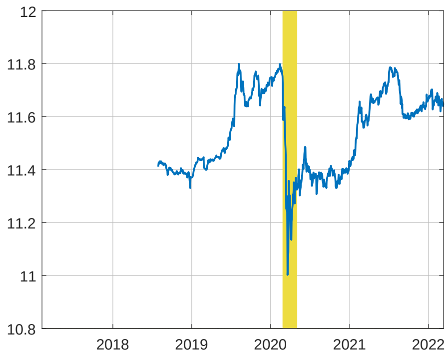

$\ln P_t$ (#58 TLR)

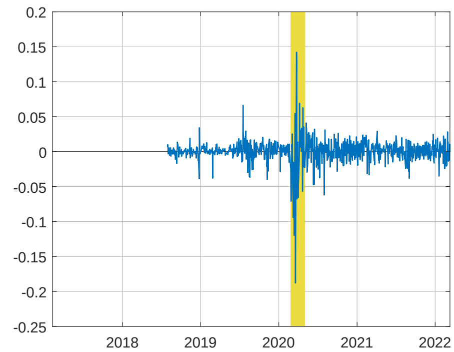

$\Delta \ln P_t$ (#58 TLR)

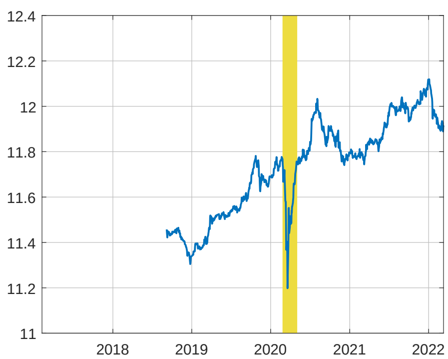

$\ln P_t$ (#59 IAL)

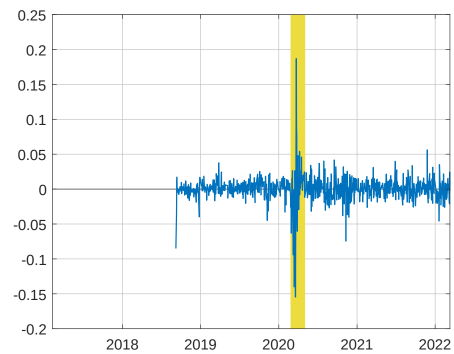

$\Delta \ln P_t$ (#59 IAL)

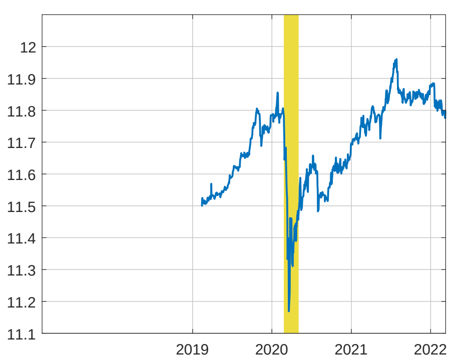

$\ln P_t$ (#60 EJR)

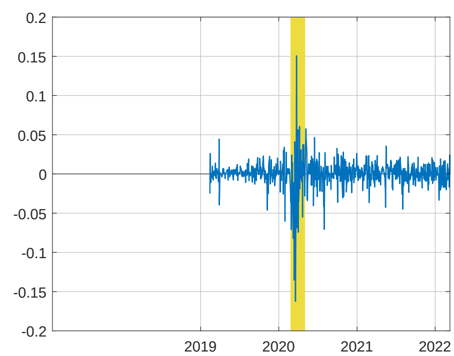

$\Delta \ln P_t$ (#60 EJR)

This figure plots the log-price $\ln P_t$ and the log-return $\Delta \ln P_t$ of individual J-REITs (#58–#60) from February 7, 2017 – March 11, 2022. The shaded area depicts the COVID-19 crisis period: February 27 – May 1, 2020. #58 TLR began being traded on July 30, 2018. #59 IAL began being traded on September 7, 2018. #60 EJR began being traded on February 13, 2019.

Figure 1: Daily stock prices and returns of J-REITs (continued)

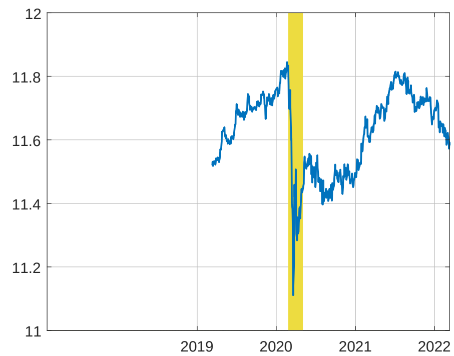

$\ln P_t$ (#61 SRE)

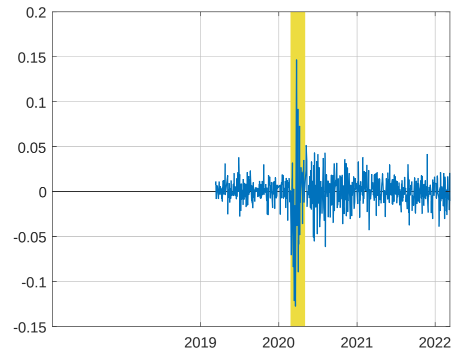

$\Delta \ln P_t$ (#61 SRE)

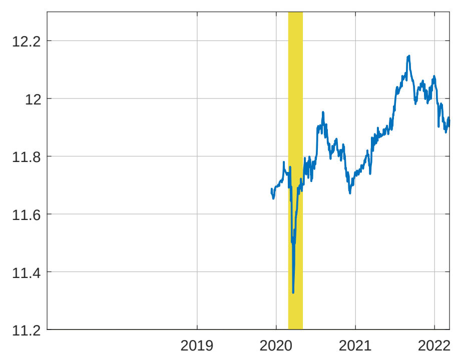

$\ln P_t$ (#62 SLR)

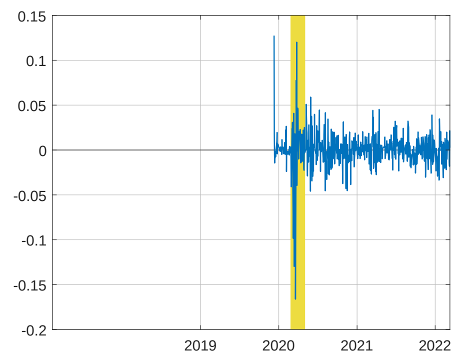

$\Delta \ln P_t$ (#62 SLR)

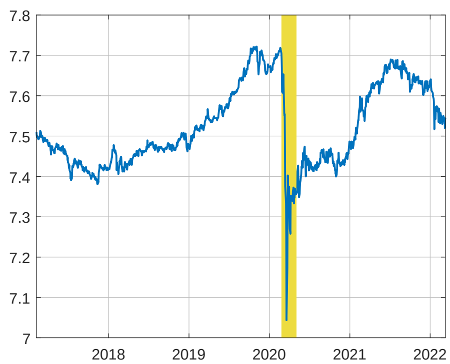

$\ln P_t^m$ (TSE REIT Index)

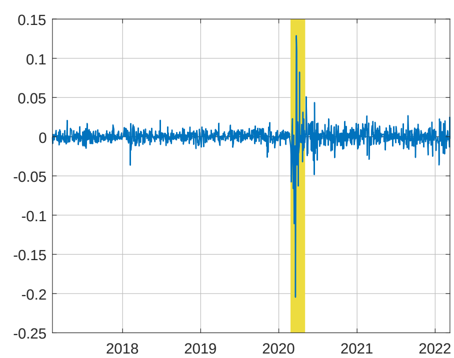

$\Delta \ln P_t^m$ (TSE REIT Index)

This figure plots the log-price $\ln P_t$ and the log-return $\Delta \ln P_t$ of individual J-REITs (#61–#62) as well as the Tokyo Stock Exchange REIT Index from February 7, 2017 – March 11, 2022. The shaded area depicts the COVID-19 crisis period: February 27 – May 1, 2020. #61 SRE began being traded on March 12, 2019. #62 SLR began being traded on December 10, 2019. In the main analysis, the TSE REIT Index is used as an auxiliary variable.

References

Brüggemann, R., C. Jentsch, and C. Trenkler (2016): "Inference in VARs with conditional heteroskedasticity of unknown form," *Journal of Econometrics*, 191, 69–85.

Capozza, D. R., and P. J. Seguin (1999): "Focus, Transparency and Value: The REIT Evidence," *Real Estate Economics*, 27, 587–619.

Cavaliere, G., L. De Angelis, A. Rahbek, and R. A. M. Taylor (2018): "Determining the cointegration rank in heteroskedastic VAR models of unknown order," *Econometric Theory*, 34, 349–382.

Hafner, C. M., and H. Herwartz (2009): "Testing for linear vector autoregressive dynamics under multivariate generalized autoregressive heteroskedasticity," *Statistica Neerlandica*, 63, 294–323.

Jentsch, C., and K. G. Lunsford (2019): "The dynamic effects of personal and corporate income tax changes in the United States: Comment," *American Economic Review*, 109, 2655–2678.